Lawrence Berkeley National Laboratory
Recent Work

Title
ROTATIONAL BANDS IN THE LIGHT ODD-MASS THALLIUM NUCLEI

Permalink
https://escholarship.org/uc/item/8kc2r43q

Authors
Newton, J.O.
Stephens, F.S.
Diamond, R.M.

Publication Date
1973-11-01

eScholarship.org Powered by the California Digital Library
University of California

Submitted to Nuclear Physics

RECEIVED
LAWRENCE
RADIATION LABORATORY

MAY 15 1974

LIBRARY AND
DOCUMENTS SECTION

LBL-2333
Preprint

ROTATIONAL BANDS IN THE LIGHT ODD-MASS THALLIUM NUCLEI

J. O. Newton, F. S. Stephens and R. M. Diamond

November 1973

Prepared for the U. S. Atomic Energy Commission
under Contract W-7405-ENG-48

TWO-WEEK LOAN COPY

This is a Library Circulating Copy which may be borrowed for two weeks. For a personal retention copy, call Tech. Info. Division, Ext. 5545

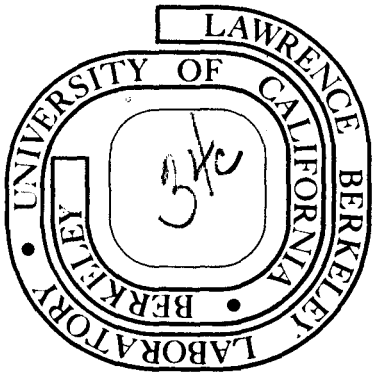

LBL-2333

DISCLAIMER

This document was prepared as an account of work sponsored by the United States Government. While this document is believed to contain correct information, neither the United States Government nor any agency thereof, nor the Regents of the University of California, nor any of their employees, makes any warranty, express or implied, or assumes any legal responsibility for the accuracy, completeness, or usefulness of any information, apparatus, product, or process disclosed, or represents that its use would not infringe privately owned rights. Reference herein to any specific commercial product, process, or service by its trade name, trademark, manufacturer, or otherwise, does not necessarily constitute or imply its endorsement, recommendation, or favoring by the United States Government or any agency thereof, or the Regents of the University of California. The views and opinions of authors expressed herein do not necessarily state or reflect those of the United States Government or any agency thereof or the Regents of the University of California.

NUCLEAR REACTIONS $^{182}W(^{14}N,5n\gamma)^{191}Tl$, E = 86-105 MeV; $^{181}Ta(^{16}O,6n\gamma)^{191}Tl$, E = 109-122 MeV; $^{197}Au(\alpha,8n\gamma)^{193}Tl$, E = 93-116 MeV; $^{184}W(^{14}N,5n\gamma)^{193}Tl$, E = 82-89 MeV; $^{181}Ta(^{16}O,4n\gamma)^{193}Tl$, E = 79-98 MeV; $^{181}Ta(^{19}F,7n)^{193}Pb$, E = 110-130 MeV; $^{197}Au(\alpha,6n\gamma)^{195}Tl$, E = 68-80 MeV; $^{188}Os(^{11}B,4n\gamma)^{195}Tl$, E = 57 MeV; $^{186}W(^{14}N,5n\gamma)^{195}Tl$, E = 85-93 MeV; $^{181}Ta(^{19}F,5n)^{195}Pb$, E = 86-105 MeV; $^{185}Re(^{14}N,4n)^{195}Pb$, E = 74 MeV; $^{197}Au(\alpha,4n\gamma)^{197}Tl$, E = 42-59 MeV; $^{190}Os(^{11}B,4n\gamma)^{197}Tl$, E = 57 MeV; $^{187}Re(^{14}N,4n)^{197}Pb$, E = 74 MeV; $^{186}W(^{16}O,5n)^{197}Pb$, E = 89 MeV; measured $\sigma(E;E_{ce},E_{\gamma},\theta_{\gamma})$, $\gamma\gamma$-coin. $^{191,193,195,197}Tl$ deduced levels, J,π,cc,γ-mixing, oblate shape. Natural and enriched targets. Ge(Li) and Si(Li) detectors.

RADIOACTIVITY $^{193,195,197}Pb$; measured E_{γ}, I_{γ}, E_{ce}, I_{ce}, $T_{1/2}(\beta)$ $\gamma\gamma$-coin. $^{193,195,197}Tl$ deduced levels, J,π,cc, log ft. Ge(Li) and Si(Li) detectors.

LBL-2333

ROTATIONAL BANDS IN THE LIGHT ODD-MASS THALLIUM NUCLEI*

J. O. Newton†, F. S. Stephens, and R. M. Diamond

Lawrence Berkeley Laboratory
University of California
Berkeley, California 94720

November 1973

Abstract

The odd-mass nuclei $^{191-197}$Tl have been formed in a variety of (HI,xn) reactions and studied by in-beam spectroscopic techniques. The decay of the high-spin Pb isomers, also formed in (HI,xn) reactions, leading to $^{193-197}$Tl have also been investigated. Evidence is presented for the existence of levels of the previously proposed $9/2^-[505]$ rotational bands in the nuclei. Tentative evidence is given for the existence of oblate rotational bands, based on the $13/2^+[606]$ state, in $^{191-195}$Tl.

*Work performed under the auspices of the U. S. Atomic Energy Commission.

†Present Address: Department of Nuclear Physics, Australian National University, Canberra, Australia.

1. Introduction

In the light odd-mass thallium nuclei, Diamond and Stephens[1]) identified low-lying $9/2^-$ isomeric states having excitation energies varying systematically with mass number. The interpretation of these states was a puzzle for some years, since the only low-lying state of high spin predicted by the simple spherical shell model is the $11/2^-$ hole state arising from the $h_{11/2}$ orbit. More recently Newton et al.[2]) reported an in-beam study of ^{199}Tl using the ^{197}Au(α,2nγ) ^{199}Tl reaction, and also included a preliminary report of some of the present work. They found the systematic occurrence of $11/2^-$, $13/2^-$ and $15/2^-$ states above the $9/2^-$ isomers. The proposed interpretation was that these states formed a rotational band based on the $K = 9/2^-[505]$ state arising from the $h_{9/2}$ orbital. Reasons were given why the thallium nuclei might be expected to have oblate deformation in this band, as required by the interpretation, and why the $K = 9/2^-$ state should be low-lying. More recently, evidence has accumulated that rotational bands, based on states arising from high-spin orbitals, are more commonly seen in supposedly spherical nuclei than previously thought[3]).

Here we report on the level schemes of the odd-mass nuclei $^{191\text{-}197}$Tl, as deduced from several in-beam (HI,xnγ) reactions and from the decay of the high-spin lead isomers. Tentative evidence is presented for the existence of another rotational band, based on the $K = 13/2^+[606]$ state arising from the $i_{13/2}$ orbital.

2. Experimental Method

The decay of excited states in the thallium isotopes was studied through gamma-rays and conversion electrons. A variety of heavy-ion, xn reactions was used to form the thallium isotopes, either directly in-beam or via radioactive isotopes decaying to them. The Berkeley HILAC provided the heavy-ion beams, and in one case (^{197}Pb) the Manchester University LINAC was used. The α-particle beams, with energies up to 116 MeV, were obtained from the Berkeley 88" Cyclotron. The general methods of measurement were the same as described in the paper on ^{199}Tl, ref [2]).

The ^{181}Ta and ^{197}Au targets were metal foils, either thick or rolled to ∿5 mg/cm^2 for the γ-ray measurements or to ∿1 mg/cm^2 for the conversion-electron studies. The targets of separated tungsten and osmium isotopes were made by glueing the fine metalic powders onto lead or uranium backings, respectively, with a dilute solution of Duco-cement in amyl acetate. The backing and cement did not significantly contribute to the γ-radiation from the target, but impurities in the separated isotopes sometimes did.

The method of detection of the conversion electrons in the single-gap wedge spectrometer used in the earlier measurements[1,2]) was improved by replacing the anthracene crystal with a cooled Si(Li) detector. Because of better resolution and less sensitivity to fast neutrons, the spectra had much higher peak-to-background ratios than previously. The electron pulses were selected by a biased amplifier, followed by a single-channel analyser. At each step of the magnet current, the bias was changed proportionately, so that the pulses out of the biased amplifier were roughly constant as the magnetic field changed. Of course, they would not be exactly constant, both because electron energy is

not exactly proportional to the field and because the field is not exactly proportional to the magnet current. In order to improve on this linear interpolation, the pulses from the biased amplifier were passed through a variable-gain amplifier to a pulse-height analyser fitted with a digital stabilizer. This, by varying the gain of the amplifier, kept the peak from the solid-state detector within a chosen set of channels. Thus it was possible to keep the pulses from the focussed electrons accurately constant in height at the input to the pulse-height analyser. To minimize dead-time losses, a single-channel analyser, with appropriate window width, was connected at this point and its output scaled.

A solenoidal electron spectrometer was used to study the conversion electrons from ^{195}Pb decay between the beam pulses. The electrons were detected in a cooled Si(Li) detector. The purpose of the solenoidal magnetic field was to prevent scattered heavy-ions from reaching the detector and to reduce the solid angle for γ-ray detection relative to that for electron detection. The efficiency of this device varied somewhat with electron energy.

The measurements on the decay of the lead isotopes were made by bombarding the appropriate targets for about a half-life and then observing, with multichannel analysers, the change in the γ-spectra with time. The half-lives could be obtained after correcting the spectra for dead-time loss. The log ft values for decay to the states whose population was observed were deduced as follows. It was assumed that at least 80% of the observed decay arose from the high-spin Pb isomer, as would be expected in (HI,xn) reactions. It was also assumed that all of the decay of the high-spin isomer proceeded finally through the $3/2^+$ first excited state to the ground state of the Tl daughter. The fractional feeding to the various populated states could then

be estimated by taking into account appropriately the observed γ-ray strengths. Since not all of the decaying γ-rays were observed or could be placed in the decay schemes, the fraction of feeding to a given state must necessarily be an upper limit and hence the deduced log ft value a lower limit. The decay energies of the high-spin Pb isomers were deduced from the tabulation of Wapstra and Gove[4]), and from the systematics of the separation energies between the low- and high-spin isomers. An error of ± 1 MeV was allowed on these values. From the systematics of the heavier Pb isotopes, it was assumed that the high-spin isomer corresponded to a $13/2^+$ state.

3. Results and Level Schemes

Level schemes were deduced from coincidence relationships, energy sums and intensity flows. Spin assignments for the levels were determined from the measured conversion coefficients, from log ft values and from the γ-ray angular distributions, taking into account empirical attenuation coefficients. The fact that in a (HI,xnγ) reaction a state of a given spin is usually very weakly populated if its energy exceeds that of the yrast level of the same spin by more than about 500 keV[5]) was useful in restricting the spin values. Full details of the methods used for the establishment of the level schemes are given in the ^{199}Tl paper[2]).

3.1. THE NUCLEUS ^{193}Tl

The in-beam γ-rays from the decay of ^{193}Tl were studied through the following reactions: ^{181}Ta(^{16}O,4nγ)^{193}Tl at bombarding energies of 79, 84, 89 and 98 MeV; ^{184}W(^{14}N,5nγ)^{193}Tl at 82, 86, and 89 MeV; ^{197}Au(^{4}He,8nγ)^{193}Tl at 93, 104, and 116 MeV. The first of these reactions at 84 MeV gave the best spectra and was used for the angular distribution measurements. A typical

spectrum is shown in fig. 1. Gamma-gamma coincidences were measured and a spectrum, taken in coincidence with the 392 keV line, is given in fig. 2. The conversion-electron spectrum obtained with the aid of a wedge-gap spectrometer is shown in fig. 3. In Table 1 are listed the gamma-rays which we attribute to the decay of excited states in ^{193}Tl, together with their conversion coefficients measured at 90° to the beam direction, the measured angular distribution coefficients, and the degree of confidence in the assignments. Coincidence relationships between the observed γ-rays are given in Table 2.

A somewhat rough measurement of the decay of ^{193}Pb into ^{193}Tl was also made. The ^{193}Pb was produced by the ^{181}Ta(^{19}F,7n)^{193}Pb reaction, for which 124 MeV was found to be the optimum bombarding energy. The only two lines which we could definitely assign to the decay of ^{193}Pb were at 392 and 366 keV. The latter follows the decay of the 2.1 min $9/2^-$ isomer in ^{193}Tl. The half-lives for these two γ-rays were found to be 5.0 ± 0.6 min and 5.8 ± 0.3 min, respectively. These values are consistent with most of the 366 keV strength coming via the ^{193}Tl $9/2^-$ isomeric state, which must be fed through the high-spin ^{193}Pb isomer. A 332 keV γ-ray, which decayed with a 10.5 ± 1 min half-life, was also seen. A γ-ray of the same energy occurs in the in-beam spectrum and by analogy with the decays of ^{195,197}Pb (sections 3.2, 3.3) would be expected in ^{193}Pb decay. The longer half-life might mean that it is mixed with a line from a longer-lived nuclide. The relative intensities of the 392, 366 and 332 keV lines were found to be 35 ± 2.5, 100 and ⩽ 13 respectively.

3.1.1. Level positions.

The proposed level scheme for ^{193}Tl is shown in fig. 4. The energy x of the E3 isomeric transition depopulating the $9/2^-$ state is only known to be

less than 25 keV[1]), hence the energies of the states whose γ-decay eventually ends up in the 9/2 state are uncertain by this amount. In the discussion below we have, for brevity, not written +x after each level energy; however, it should be understood on all ^{193}Tl level energies (except the 365.3 keV level) and, as a reminder, is explicitly written in fig. 4.

From the coincidence relationships, precise energy sums, and measured intensities we can establish levels at 757.6 keV and 1081.3 keV with fair certainty. As can be seen in fig. 2, the strong 716 keV γ-ray is clearly not in coincidence with the 392 keV γ-ray, consistent with this interpretation. The level at 1512.1 keV is less definite. It is established by an accurate energy sum and by the fact that the 431 keV γ-ray is in coincidence with the 324 and 392 keV γ-rays. The poor statistical accuracy of the measured coincident intensity of the 754 keV line is not sufficient to establish that it is in coincidence with the 392 keV line, but is consistent with it being so. All of the other measured singles and coincident intensities are consistent with the above scheme. The level at 1833.0 keV is established by means of an accurate energy sum and by the 321 keV γ-ray being in coincidence with the 392 and 431 keV γ-rays. Other coincident intensities have too poor statistical accuracy to give definite information. The 269 keV γ-ray is most probably in coincidence with the 324 and 716 keV transitions and also with the weaker 202 and 208 keV transitions, which are, however, probably not in coincidence with each other. From this it seems likely that there are levels at 1350.2, 1552.5, and 1558.1 keV.

Another set of γ-rays is in coincidence with the 392 keV transition, but only weakly or not at all with the other transitions from the levels proposed above. These are the 97, 108, 126, 162, 317, 406, 467, and 736 keV γ-rays. The 736 keV γ-ray is easily the strongest of the set and therefore seems

most likely to arise from a level at 1493.2 keV and feed directly the 757.6 keV level, which decays by means of the 392 keV transition. The 126 and 406 keV γ-rays are most probably in coincidence with the 736 keV transition, and also with the 162, 317 and 467 transitions, which are also in coincidence with one another. Unfortunately the statistical accuracy of our measurements is not good enough to tell whether or not the latter three γ-rays are in coincidence with the 736 keV transition. Any of these which are not in coincidence with it must be involved in a cascade of γ-rays, presumably depopulating the 1493.2 keV state and leading to the 757.6 keV state. We do not find any satisfactory energy sums which might indicate such a cascade, though it is always possible that one of its members has not been observed. On balance it seems more likely therefore that these γ-rays are in coincidence with the 736 keV transition. One slight doubt about the proposed 1493.2 keV level arises because the angular distribution of the 126 keV γ-ray is not known and neither is its multipolarity. It is just possible, if it is a pure M1 transition, that its intensity could be equal to, or slightly exceed, that of the 736 keV transition, in which case it would follow this transition. The multipolarity of the 126 keV transition cannot be M2 or higher because its lifetime would then be longer than about 1 μsec, which is much longer than the coincidence resolving time. In the following we shall assume the assignment of the 1493.2 keV level to be correct. Apart from noting that the 317 keV line must be double because it is in coincidence with itself (Table 2), further discussion of this part of the decay scheme will be deferred until Section 4.

The 672.5 keV γ-ray does not appear to be in coincidence with any others. Because it is a fairly strong transition, it seems most likely that it feeds the isomeric state, rather than the low-spin ground or first excited states. If this hypothesis is correct, it establishes a level at 1037.8 keV.

3.1.3. Spin assignments.

The states at 758, 1081 and 1512 keV have great similarities in their relative spacings, decay modes and γ-ray angular distributions to those[2]) of the 1118, 1450, and 1867 keV states in ^{199}Tl. The evidence leading to their spin assignments is nearly identical to that for the corresponding ^{199}Tl assignments, apart from the following two points. We were not able to measure the K/L ratio for the 323 keV transition and so it is not possible, as it was in ^{199}Tl, to distinguish between the M1 + E2 and E1 + M2 possibilities for this transition by this method. Further, we do not have detailed excitation function data, which can give useful evidence on the spins of the states, particularly in (α,2n) reactions.

For the 758 keV state, the angular distribution and conversion data allow 11/2±, and less likely 7/2± for which the A_2 coefficient of the 392 keV angular distribution is two standard deviations too large. Indeed, the latter possibility can be ruled out on the grounds that the 392 keV γ-ray is the strongest in-beam γ-ray, so it can hardly come from a 7/2 state 392 keV higher than a 9/2 state, when these are made in a (HI,xnγ) reaction. Further, it is populated in the decay of ^{193}Pb with a log ft value of 6.1 ± 0.3, indicating that the transition is most likely to be first forbidden, although an allowed transition is not excluded. Since we would expect to make mainly the high-spin isomer of ^{193}Pb, and since the high-spin isomer most likely has a spin of $13/2^+$, this again fairly strongly rules out the 7/2 possibility and favors $11/2^-$ for the spin of the 758 keV state. An $11/2^+$ assignment is unlikely because it would require an unusually large (about 30%) M2 component in the E1/M2 transition. By essentially similar arguments to those used for establishing the possible spin of the 1450 keV state in ^{199}Tl, we deduce that the spin of the 1081 keV state, as allowed by

the angular distribution and conversion data, is $9/2^+$ or $13/2^-$. In view of the strong population of the state, which is 754 keV above the $9/2^-$ state, the $13/2^-$ possibility seems most likely.

Again arguing by analogy with the ^{199}Tl case, consideration of the angular distributions and conversion coefficients of the 754 and 431 keV transitions, together with the above conclusions, leads to the following possibilities for the spins of the 758, 1081, and 1512 keV states, respectively: (i) $11/2^-$, $13/2^-$, $15/2^-$ or $11/2^+$; (ii) $11/2^+$, $13/2^-$, $15/2^+$ or $11/2^-$; (iii) $11/2^-$, $9/2^+$, $11/2^-$ or $7/2^-$; (iv) $11/2^+$, $11/2^-$ or $7/2^+$. For the reasons already given, (i) seems most likely to be correct, with (ii) somewhat unlikely, and (iii) and (iv) very unlikely. For (i) and (ii) the 11/2 possibility for the 1537 keV state is unlikely on intensity grounds. Hence the most probable assignments for the three states are 11/2, 13/2 and 15/2 respectively, with negative parity most likely. In the arguments below we assume the $11/2^-$ and $13/2^-$ assignments for the 758 and 1081 keV states to be correct.

For the state at 1833 keV which decays to the 1512 and 1081 keV states, we merely comment that the angular distribution and conversion data are consistent, within the rather large errors, with the 321 keV γ-ray being M1 and the 752 keV γ-ray being a stretched E2 transition, as would be required if the 1833 keV state were $17/2^-$.

A slight reservation should be made to the preceding arguments. Namely, in the angular distribution measurements, the 321 and 324 keV, the 464, 467 and 469 keV and 752 and 754 keV lines were not fully resolved. As far as can be seen, they have similar distributions, but we cannot be completely certain of this.

The 1350 keV state decays via the 269 keV transition to the $13/2^-$ 1081 keV state. The angular distribution shows that it is not a stretched $\Delta I = 2$ transition, so

the spin can be 11/2, 13/2 or 15/2 with either parity. Of these possibilities 15/2 is slightly preferred, since no decay is observed to the 758 keV state.

The 1038 keV state decays to the $9/2^-$ 365 keV state by means of the 672 keV transition. Its angular distribution is consistent with the state having any spin between 5/2 and 13/2. Since the transition is fairly strong, spins of 9/2 and below would seem very unlikely.

The state at 1493 keV decays to the $11/2^-$ 782 keV state via the 736 keV transition. The angular distribution of this transition excludes the possibility of its being a stretched E2, and the conversion coefficient seems only consistent with E1 + (3.5±2)% M2. An assignment of $11/2^-$ would be possible if the transition were mainly E2, which in itself seems most unlikely, but the conversion coefficient would then be more than two standard deviations from the measured value. These data allow $9/2^+$ and $13/2^+$ assignments. However, because of the great strength of the 736 keV transition, the $13/2^+$ possibility seems almost certain to be the correct one.

The placement of the 406 keV and 467 keV γ-rays will be discussed in Section 4. Here we comment that their conversion coefficients and angular distributions exclude them from being stretched $\Delta I = 2$ transitions or $I \rightarrow I$ transitions. The data are consistent with them being mainly M1(+ ∿10% E2) or E1 + ∿40% M2 transitions. Of these, the former seems to be more likely.

3.2. THE NUCLEUS ^{195}Tl

Gamma rays following the direct production of ^{195}Tl were observed with the following reactions: ^{186}W(^{14}N,5nγ)^{195}Tl at 85 and 93 MeV, including an angular distribution measurement at 85 MeV; ^{197}Au(α,6nγ)^{195}Tl at 68, 74, and 80 MeV; ^{188}Os(^{11}B,4nγ)^{195}Tl at 57 MeV. The data on the last of the above

reactions were taken at a later date and owing to improved detector resolution, are of better quality. None of the spectra were of as good a quality as those obtained in the $^{197}Au(\alpha,2n\gamma)^{199}Tl$ and $^{181}Ta(^{16}O,4n\gamma)^{193}Tl$ reactions. This was due to target problems in the case of the reactions on ^{186}W and ^{188}Os. These separated isotopes were in metallic powder form but contained impurities which contributed strong continuous γ-ray backgrounds as well as discrete γ-rays. The measurements on the $(\alpha,6n\gamma)$ reactions suffered from poor detector resolution. Also, for large numbers of particles emitted, the excitation functions became broader, overlapping more, and decreasing the uniqueness of the product nucleus. In spite of these problems, the use of a variety of reactions and bombarding energies to produce ^{195}Tl was valuable in enabling firm identification of its γ-rays.

The decay of ^{195}Pb into ^{195}Tl was also studied. It was produced by the $^{181}Ta(^{19}F,5n)^{195}Pb$ reaction at 97 MeV bombarding energy. An excitation function had previously been measured in order to deduce the optimum bombarding energy.

3.2.1. The in-beam measurements. A spectrum of the in-beam gamma rays from the $^{188}Os(^{11}B,4n\gamma)^{195}Tl$ reaction is shown in fig. 5. The energies, intensities and angular distribution coefficients of the gamma rays attributed to decays within ^{195}Tl are given in Table 3.

3.2.2. The decay of ^{195}Pb. A spectrum of the γ-rays, taken for the first twelve minutes after bombardment, is shown in fig. 6. In order to assign the lines and obtain the half-lives, the decay was followed for a period of 70 minutes after bombardment. The half-lives associated with the 394 keV and 384 keV gamma rays were found to be identical within the experimental errors, and the

best value was 16.4 ± 0.3 m. The 394 keV γ-ray arises from the decay of the high-spin isomer of ^{195}Pb, while the 384 keV γ-ray can arise from the decay of both states. However, as previously explained, it seems unlikely that we would make very much of the low-spin isomer.

We examined the conversion-electron spectrum from ^{195}Pb decay with a cooled lithium-drifted silicon counter, placed in a solenoidal magnetic field. The spectrum, taken between the beam pulses with a 1 mg/cm^2 Ta target, is shown in fig. 7. The strong 99 keV E3 transition in ^{195}Tl is notable. However, no other strongly converted line is seen above 55 keV. As might be expected from the systematics, this indicates that the M4 transition between the 13/2$^+$ high-spin isomer in ^{195}Pb and the 5/2$^-$ state no longer competes with the electron-capture decay of the 13/2$^+$ state.

The energies and intensities of the gamma rays from the decay of the ^{195}Pb states are shown in Table 4. The assignments were made on the basis of half-life, and the degree of confidence in them is indicated. Rather rough estimates of the K-conversion coefficients, derived from the electron data, are also given in the Table. They were obtained by assuming a value of 0.069 for that of the 384 keV transition, whose M1-E2 mixing ratio is known[1]). The values are rough because of uncertainties in the efficiency of the solenoidal spectrometer as a function of electron energy. Thus, both they and the multipolarities deduced from them must be taken with some caution. Our rough value for the intensity of the 99 keV isomeric transition suggests that it is about 75 ± 15% of that for the 384 keV transition. The results of γ-γ coincidence measurements, taken with two Ge(Li) detectors, are also given in the Table. We disagree with the recent result of Hopke et al.[6]), who also studied the decay of

^{195}Pb, that the 384 and 394 keV γ-rays are in coincidence. Our results also suggest that the 313 keV transition is M1 rather than M2, as reported by Hopke et al.[6]). Even with the mentioned uncertainty in the determination of the relative intensitites of the conversion electrons, previous experience with the solenoidal electron spectrometer suggests that our result would not be in error by more than about 30%, whereas a factor of three is required to bring it in accordance with the value appropriate to an M2 transition. Of course, the 313 keV transition could be an E1,M2 admixture.

3.2.3. Level assignments. Much the strongest line in the in-beam spectrum is that at 394 keV. Therefore, this γ-ray is most likely to feed either the ground state or the $9/2^-$ state (see fig. 8). Since it is such a strong line, the latter possibility is much more probable. We shall assume it to be correct and therefore that the 394 keV γ-ray originates from a state at 877.0 keV. A state at 1190.5 keV, from which the 313 and 708 keV γ-rays arise, is established by an energy sum and more firmly by the fact that the 394 and 313 keV gamma-rays are in coincidence in ^{195}Pb decay. The state at 1484.6 keV is established from the coincidence of the 394 and 608 keV gamma-rays in ^{195}Pb decay. An energy sum with the 313 and 429 keV lines suggests a level at 1619.6 keV. The 878.2 keV gamma-ray is seen very strongly in the decay of ^{195}Pb, but is very weak or absent in the in-beam spectrum. This suggests that it originates from a state of relatively low spin and may possibly be fed by the low-spin level of ^{195}Pb. Its strength suggests that it feeds either the 384 keV state or the 483 keV state, since the intensity of the 384 keV transition is much greater than that reaching the 483 keV state from the 394 and 708 keV transitions. However, a rather poor energy sum between the weak 493 keV line and the 384 keV line

somewhat favors it feeding the ground state. Without further information, we are not able to place any of the other lines in the decay scheme.

The information on the angular distributions of the gamma-rays from the 877 and 1191 keV states is similar to that on the gamma-rays from the 1118 and 1450 keV states in ^{199}Tl, which were assigned spins of $11/2^-$ and $13/2^-$, respectively. Similar information is available on the K-conversion coefficients, but the K/L ratio of the 313 keV transition is not known. From this information, we can deduce that the 877 keV state can be $11/2\pm$ with the 1191 keV state $9/2\pm$ or $13/2^-$, or less likely, the 877 keV state can be $7/2\pm$ with the 1191 keV state $9/2^+$. The information from the decay of ^{195}Pb can be used to eliminate some of these possibilities if we assume, as is likely, that the spins of the two ^{195}Pb states are $13/2^+$ and $3/2^-$. The log ft values of 6.2 ± 0.2 and 6.3 ± 0.2 for the decay to the 877 and 1191 keV states, respectively, indicate that the transitions are most likely to be first forbidden (not unique), though one cannot exclude the possibility of them being allowed. Thus, the only possibilities for the spins of the 877 and 1191 keV states are $11/2\pm$ and $13/2^-$, respectively, with negative parity for the 877 keV state being easily the most likely. Negative parity is also favored since otherwise the 394 and 313 keV transitions would have to be mixed E1/M2 with special mixing ratios to give approximately the same conversion coefficients as for M1 radiation. Moreover, the 30% M2 admixture needed to do this is unusually large.

The 1485 keV state decays to the 11/2, 877 keV state. The sign and magnitude of the A_2 coefficient of the 608 keV gamma-ray eliminates the 15/2 possibility for the spin, leaving $13/2^-$ and $11/2^-$ allowed by the ^{195}Pb decay. The somewhat tentative 1620 keV state feeds the $13/2^-$ and $11/2^-$ states. It may

also be fed in the decay of ^{195}Pb since a 741.9 keV γ-ray is observed which has a half-life consistent, within the rather large errors, with that for ^{195}Pb decay. A 429.1 keV γ-ray is also seen but decays with a longer apparent half-life than ^{195}Pb. This could either mean that it is not present at all in ^{195}Pb decay, or else that it is present, but another line at approximately the same energy is either growing in or decaying with a long half-life. The possible spins are 11/2, 13/2 or 15/2. However, in view of the strong population of the state and the fact that there is a 13/2 state 742 keV below, the 15/2 assignment seems most likely.

3.3.1. The nucleus ^{197}Tl. The lines attributed to the in-beam decay of ^{197}Tl, shown in Table 5, were deduced from γ-ray spectra from the ^{197}Au(^{4}He,4nγ)^{197}Tl reaction, taken at bombarding energies of 42, 52 and 59 MeV and from the ^{190}Os(^{11}B,4nγ)^{197}Tl reaction at 57 MeV. A spectrum from the latter reaction is shown in fig. 9. All the measurements were taken at 90° to the beam direction. No angular distribution, coincidence, or conversion electron measurements were made. The proposed level scheme, shown in fig. 10, is therefore necessarily more tentative than for ^{193,195}Tl.

Since the 387.7 keV γ-ray is by far the strongest in the spectrum, it must almost certainly feed the 9/2$^-$ isomeric state at 608.1 keV, indicating a level at 995.8 keV (see fig. 10). This and the level at 1303.6 keV, which is suggested by an energy sum, are in general accordance with the systematics for the odd thallium isotopes, as is a further level at 1720.0 keV, which is suggested by energy sums. It seems plausible that these may be the 11/2$^-$, 13/2$^-$ and 15/2$^-$ members of the proposed[2]) oblate rotational band. The strong 561.2 keV γ-ray seems, on the basis of intensity considerations, most likely to feed the 995.8 keV state or possibly the isomeric state. We cannot distinguish with certainty between these possibilities without coincidence measurements.

A partial study of the decay of ^{197}Pb into ^{197}Tl was made, and γ-rays with energies up to about 500 keV were observed. The ^{197}Pb was obtained through the ^{187}Re(^{14}N,4n)^{197}Pb reaction, by bombarding a natural rhenium target with 74 MeV ^{14}N. The nucleus ^{195}Pb was also produced from the reaction with ^{185}Re, but because of its shorter half-life, its decay could easily be distinguished from that of ^{197}Pb. A number of spectra were taken over a period of several hours and the lines which we attributed to the decay of ^{197}Pb are given in Table 6. The assignments of Hopke et al.[6]) are also included in the table. There are differences between the results. Some may be due to the different methods of source preparation, possibly leading to different relative amounts of high-spin isomer and ground state. A major discrepancy is their claim that the 385.6 keV line is single and does not have a 387 keV component, as indicated by the early results of Andersson et al.[7]) and by the present data (fig. 11). From a comparison of the in-beam and ^{197}Pb decay results, it appears that the high-spin isomer populates the proposed levels at 995.8 keV and 1303.6 keV. Assuming an energy of 4.0 ± 1 MeV for decay from the isomer to the ground state of ^{197}Tl, we obtain log ft values of 6.5 ± 0.25 and 6.6 ± 0.25 for the decays to the 995.8 and 1303.6 keV levels respectively. These values suggest that the transitions are first forbidden (not unique) though it cannot be excluded that they are allowed. The values could in fact be somewhat higher, since we have only considered direct population of the two states by electron capture and positron emission. These results of the ^{197}Pb decay strongly support our proposed scheme, since the $13/2^+$ isomer can only populate states with spins between 11/2 and 15/2, unless the log ft values are grossly in error, which seems unlikely. Further, negative parity seems most likely for the two states.

The $5/2^+$ level at 761.0 keV was proposed by Hopke et al. on the basis of a coincidence measurement. A $5/2^+$ level at about this energy would be expected from the systematics of the heavier Tl isotopes. We also see the 375.3 keV γ-ray from its decay but more weakly than do Hopke et al., suggesting that we make less of the low-spin ground state than they do. Over a period of about four half-lives, we were not able to detect any significant (> 5%) change in the ratio of the intensity of the 387.7 keV line, which arises only from the decay of the isomer, to that of the 385.7 keV line, which arises both from the decay of the isomer and the ground state (see fig. 10). Since 20% of the isomer decay goes to the ground state of ^{197}Pb, this implies that the ground state has a shorter half-life than the isomer or at least that it is not much longer. In our experiment it seems that, as expected, we made rather little of the ground state directly, since the total intensity of the 222.4 keV transition (including internal conversion) is about 75% of that of the 385.7 keV line.

3.4. THE NUCLEUS ^{191}Tl

In order to identify the γ-rays in ^{191}Tl, the following reactions were studied: ^{181}Ta(^{16}O,6nγ)^{191}Tl at 109, 116 and 122 MeV and ^{182}W(^{14}N,5nγ)^{191}Tl at 86, 93 and 105 MeV bombarding energy. The spectra (see fig. 12) were generally of poorer quality than for the other odd thallium nuclei, possibly because charged-particle emission is becoming important for this very neutron-deficient system. No coincidence or detailed angular distribution measurements were made. However, spectra were taken at 0° and 90° to the beam direction in order to determine which γ-rays were peaked at 0° (positive A_2) or at 90° (negative A_2). No delayed γ-ray was seen, indicating that the isomeric $9/2^-$ state has now fallen below the $3/2^+$ state. Because of the high internal-

conversion coefficient for low-energy E3 transitions, it is unlikely that the half-life of the E3 transition to the $3/2^+$ state would become significantly longer than that of 2.1 m for the < 25 keV transition in ^{193}Tl. One would therefore expect to see the $3/2^+ \rightarrow 1/2^+$ γ-ray, if the $9/2^-$ state were above the $3/2^+$ state, even if there was some competition from electron-capture decay. The information obtained from these studies is summarized in Table 7.

3.4.1. Level positions and assignments. Because of the absence of coincidence measurements and decay measurements on ^{191}Pb, the assignments are necessarily more tentative for this nucleus than for the other thallium nuclei. In ^{191}Tl we again see that the strongest in-beam γ-ray (387.6 keV) has an energy of approximately 390 keV and is strongly peaked at 90°, as in $^{193\text{-}199}$Tl. It is very likely, therefore, that this transition feeds the $9/2^-$ state. We have no information about the excitation energy of the $9/2^-$ state above the ground state, apart from extrapolating from the systematics of the heavier thallium isotopes. Therefore in the following we shall measure excitation energies relative to that of the $9/2^-$ state, though these energies are followed by +x in fig. 13 as a reminder that the energy above the ground state is not known. Our first proposed level is at 387.6 keV (see fig. 13) and by analogy with $^{193\text{-}199}$Tl we would expect it to be the $11/2^-$ level. An energy sum between the 387.6 keV γ-ray and the strong 325.6 keV γ-rays suggest a level at 713.2 keV. The energies and angular anisotropies are closely analogous to those for the decay of the $13/2^-$ level in $^{193\text{-}199}$Tl. The data on the higher-energy γ-rays are not of sufficient accuracy to justify establishing levels by energy sums. From the systematics of the other thallium nuclides (see Table 8), the 434.5 keV γ-ray, which is peaked at 90°, seems the best candidate for the $15/2^-$ to $13/2^-$ transition. If this is correct it arises from a level at 1447.7 keV.

3.5. SUMMARY

In each of the studied nuclei we have observed a band of states with similar spacings and with spins, increasing with excitation energy, which are most probably $9/2^-$, $11/2^-$, $13/2^-$, ... These states decay by M1 +E2 cascade transitions and E2 crossover transitions. The E2/M1 amplitude mixing ratio δ is negative in all cases and of similar magnitude to that observed in ^{199}Tl for decay of the corresponding states. We also observe γ-rays arising from other states, whose interpretation will be considered in the next section.

4. Discussion

A preliminary report of the systematic occurrence of $11/2^-$, $13/2^-$ and $15/2^-$ states above the $9/2^-$ isomeric state in the lighter odd-mass thallium nuclei was given[2]) in the ^{199}Tl paper. An explanation was given in terms of a rotational band based on the $9/2^-$ [505] Nilsson state. This state, derived from the $h_{9/2}$ orbit, can be low lying if the thallium nuclei have oblate deformation and if there is sufficient gain in pairing energy, due to reduced blocking, when the odd proton is excited up to the next shell. This conclusion was supported by theoretical evidence on the deformation potentials for the doubly-even mercury nuclei[8]) and by empirical evidence on the gain in pairing energy[9]). The observed departure from simple rotational energy spacings was of the right form and order-of-magnitude as expected from the strong Coriolis mixing between states derived from the $h_{9/2}$ orbit. Also the E2 branching ratio from the $13/2^-$ to the $11/2^-$ and $9/2^-$ states in ^{199}Tl was consistent with this explanation. Later, Nakai[10]) pointed out that the sign of the E2/M1 mixing ratios between the states of the proposed band supported the hypothesis of oblate deformation. Recently Stephens *et al.*[11]) have carried out computer

calculations in which they have diagonalized the matrix of the Coriolis interaction operating on all the states arising from the $h_{9/2}$ orbit. These calculations show more quantitatively that the above proposed explanation for this band in the odd-mass thallium nuclei appears to be correct.

In addition to the states mentioned above, other high-spin states are seen, though they exhibit no obvious systematic behavior. In order to gain further insight, let us consider, in a simple way, the high-spin states which may be expected to exist below about 3 MeV excitation energy in the odd-mass thallium nuclei. When the nuclei are spherical, these are likely to arise principally from three-quasiparticle states or from weak coupling between one of the odd-proton orbitals and collective states of the core. The nearby orbitals in the occupied shells are $s_{1/2}$, $d_{3/2}$ and $h_{11/2}$ for the protons and $p_{1/2}$, $f_{5/2}$, $p_{3/2}$, $i_{13/2}$ and $h_{9/2}$ for the neutrons. By analogy with ^{207}Tl the only low-lying one-quasiparticle state of high spin, the $(h_{11/2})^{-1}$ state, would be expected at about 1.3 MeV excitation energy. We confine ourselves to three-quasiparticle states of the [2ν,1π] type, since [3π] states are expected to be at very high excitation energy. Here we can be guided by empirical information on the [2ν] states in the doubly-even Hg and Pb nuclei (see fig. 14, showing systematics of various levels in the Hg and Tl nuclei). In both cases, 5^- and 7^- states, probably attributable mainly to the configuration [$i_{13/2}$, $p_{3/2}$ and $p_{1/2}$], occur systematically[12-17]) at roughly constant excitation energies of about 1.8 and 2.1 MeV, respectively. In addition 9^- states are reported in ^{200}Hg and $^{194-204}$Pb at about 2.2 MeV. Even-parity [2ν,1π] states can be obtained by coupling these [2ν] states with the $(h_{11/2})^{-1}$ proton state, whilst odd-parity states can be obtained by coupling with the $s_{1/2}$ and $d_{3/2}$

proton states. Assuming weak coupling, we can deduce the approximate positions of the $[2\nu,1\pi]$ states from the known energy differences of the single-proton states. These are indicated in fig. 15.

Similarly we can estimate the positions of the states obtained by coupling between the odd-proton states and the collective states of the core (see fig. 14). The existence of 2^+ and 4^+ states have been reported in $^{190-202}$Hg and $^{194-204}$Pb and 6^+ states in $^{190-200}$Hg, ref. [12-19]). Taking the mean of the Hg and Pb results where possible, we might estimate the energies of the 2^+, 4^+ and 6^+ core states to be around 700, 1300 and 1800 keV, respectively.

Whilst we cannot expect to get a precise representation of the energies of the high-spin states by the above method and certainly some states will not have been included, it should at least give a good guide to their general distribution in this region of excitation energy. Roughly, this should be independent of mass number. In fig. 15 two notable features can be seen. For spins $\gtrsim 15/2$, the density of odd-parity states is from three to four times higher than that of even-parity states. Also, by comparison with the partial level schemes of ^{193,199}Tl, (fig. 15), one sees that members of the $K = 9/2^-$ rotational band have been identified, presumably because strongly populated, only when there are not many nearby levels of similar spin. This result, although expected, gives some confidence that our estimates of the positions of the states are not seriously in error.

We now consider possible non-spherical states, of which the $K = 9/2^-$ band is an example. The only other band which might be formed in the same way and also produce high-spin states at low-excitation energy is the oblate $K = 13/2^+$ band arising from the $i_{13/2}$ orbital. In ^{209}Bi the $h_{9/2}$ and $i_{13/2}$ states are

separated by 1.6 MeV. Also, from Nilsson's calculations[20]), one expects a more rapid decrease in energy with increasing oblate deformation for the $K = 13/2^+$ [606] state, than for the $K = 9/2^-$ state. This ranges from about 0.3 MeV for ^{199}Tl to 0.4 MeV for ^{193}Tl. Hence the $13/2^+$ state would be expected at an excitation energy of about 1.2 to 1.3 MeV above the $9/2^-$ state, or about 1.4 and 2.05 MeV above the ground state for ^{193}Tl and ^{199}Tl, respectively. From fig. 15 we see that the possible $K = 13/2^+$ state is considerably lower in energy than spherical states of the same spin and either parity in ^{193}Tl, but not ^{199}Tl. Hence one is much more likely to observe γ-rays from strongly populated states of the deformed $K = 13/2^+$ band in the more neutron-deficient nuclei such as ^{193}Tl, than in ^{199}Tl. In addition, we might expect such a $K = 13/2^+$ band to be perturbed from the normal rotational spacings in a similar manner, but to a larger extent, than is the $9/2^-$ band. This is because the Coriolis matrix elements coupling the states arising from a given shell-model orbital are larger, the higher the angular momentum of the orbital. For the same reason, the decoupling parameter of the $K = 1/2$ band, which gives rise to the irregular spacings, is also larger; the Nilsson values for these are +4.7 and +6.9 for the states arising from the $h_{9/2}$ and $i_{13/2}$ orbitals, respectively.

A strongly populated $13/2^+$ state is seen in ^{193}Tl at an excitation energy of 1493.2 keV, quite close to our roughly estimated 1.4 MeV for the $I = K = 13/2^+$ state. Because there are no energy sums which might guide us in placing the energy levels which decay finally to the 1493.2 keV level, we did not discuss possibilities for these levels in Section 3.1.1. However, we shall now do this with the possibility of a $K = 13/2^+$ band in mind. From intensity considerations, either the 406 keV or the 126 keV transition (if M1) could feed the 1493.2 keV level (see Section 3.1.1. and Tables 1 and 2). If these

transitions do arise from a K = $13/2^+$ band, then we would expect to have the 406 keV transition lowest. Thus there should be levels at 1899.5 keV ($15/2^+$) and 2025.4 keV ($17/2^+$). Similarly, it is plausible that there should be levels at 2492.2 keV ($19/2^+$) and 2653.8 keV ($21/2^+$) from which the 467 and 162 keV γ-rays arise, though the experimental evidence in favor of these is not quite so strong.

The angular distributions and conversion coefficients of the 406 and 467 keV transitions are certainly in accordance with this interpretation, which requires them to be M1, with a small E2 admixture, and negative sign for the amplitude mixing ratio δ[10]). The calculations of Stephens et al.[11]) suggest that for $|\beta| \lesssim 0.15$ the energies of the I = K + 1 → I = K transitions, in these strongly perturbed bands with oblate deformation, should be approximately equal to those of the corresponding $2^+ \rightarrow 0^+$ transitions in the ground-state bands of the doubly-even Hg nuclei. Also the energies of the K + 3 → K + 1 transitions should be close to those of the $4^+ \rightarrow 2^+$ transitions. These comparisons are made in Table 8 for the $9/2^-$ bands and for the proposed $13/2^+$ band. In all cases the agreement with this prediction is quite good.

A possible objection to the proposed $13/2^+$ band is that no E2, I + 2 → I, crossover transitions are observed, whereas they are strong in the $9/2^-$ band. Though a Coriolis mixing calculation would be required to establish this point with certainty, it is easy to show that it is very unlikely that the crossover transitions would have been observed in our experiment. For a given Nilsson state, the reduced M1 transition probability is proportional to G_{M1}^2, where G_{M1} is given by[20])

$$G_{M1} = \sum_{\ell,\Lambda} a_{\ell\Lambda}^2 \; (-)^{\Sigma-1/2} \; (g_s - g_R) + 2\Lambda(g_\ell - g_R) \quad . \qquad (1)$$

Here the $a_{\ell\Lambda}$ are the amplitudes for the wave function in the $|N\ell\Lambda\Sigma>$ representation[20]). The component Σ of spin along the symmetry axis is predominantly +1/2 for levels arising from the $i_{13/2}$ orbital and -1/2 for those from the $h_{9/2}$ orbital. Hence G_{M1} is much larger for the $i_{13/2}$ levels. Taking $g_s = 0.6 g_s(\text{free})$ and $g_R = 0.3$ we find that $G_{M1}^2(i_{13/2}) \approx 7 G_{M1}^2(h_{9/2})$. Assuming, as is almost certainly the case, that the intrinsic quadrupole moments of the two bands are nearly equal, and that the relative M1 strengths in the perturbed bands are proportional to the relative values of the G_{M1}^2, we deduce that the intensity of the 17/2 → 13/2 E2 crossover transition is just possibly observable, but that the crossover transitions from higher spin states in the $13/2^+$ band should be well below the limits of what we could observe in these measurements.

The postulated $K = 13/2^+$ band in ^{193}Tl therefore seems to be in accord with our measurements, though they do not prove its existence. It would be of considerable interest to extend these measurements and attempt to do this. If the band is strongly populated in ^{193}Tl, it should be even more so in ^{191}Tl and somewhat less so in ^{195}Tl. Unfortunately, neither of these two nuclei were studied as carefully as was ^{193}Tl, hence we are only able to proceed in a speculative way by analogy with ^{193}Tl. In ^{191}Tl, the strong 614.2 keV γ-ray might well be expected to feed the $11/2^-$ state from intensity considerations and therefore arise from the decay of the $13/2^+$ state. Likewise the strong 405.0 keV γ-ray might be the $15/2^+ \rightarrow 13/2^+$ transition. In ^{195}Tl the situation is even less clear, but the best candidates for the $13/2^+ \rightarrow 11/2^-$ and $15/2^+ \rightarrow 13/2^+$ transitions are the 848.1 and 458.9 keV γ-rays, respectively,

though the latter seems somewhat higher in energy than one might expect (see Table 8). The positions of the $13/2^+$ states deduced from these speculative considerations are roughly in accord with expectations (see fig. 14).

5. Conclusion

We have shown that low-lying $K = 9/2^-$ bands with oblate deformation occur systematically in the light odd Tl nuclei. These are probably the best-developed rotational bands known to occur in nuclei with oblate shapes. At first glance, their occurrence in Tl nuclei seems very surprising, but it can be shown that a combination of the deforming tendency of the $9/2^-$ [505] Nilsson orbital, the gain in pairing energy, and the very soft deformation potentials calculated for the Hg nuclei could be expected to produce such bands. We have probably also identified very analogous oblate $13/2^+$ [606] bands in some of these Tl nuclei. This type of behavior could be expected to occur as a general feature just below closed shells if the potential energy as a function of deformation for the even-even core nucleus is sufficiently flat in the region of zero deformation. Whether this happens in other regions is at present an open and interesting question.

Acknowledgments

We would like to thank Dr. S. D. Cirilov for help with many aspects of this work, and also the operating crew of the HILAC for furnishing so patiently the variety of heavy-ion beams of different energies required.

References

1) R. M. Diamond and F. S. Stephens, Nucl. Phys. 45 (1963) 632

2) J. O. Newton, S. D. Cirilov, F. S. Stephens and R. M. Diamond, Nucl. Phys. A148 (1970) 593

3) F. S. Stephens, Proceedings of the International Conference on Nuclear Physics, Munich, Vol. II, ed. by J. de Boer and H. J. Mang, North-Holland, American Elsevier (1973)

4) A. H. Wapstra and N. B. Gove, Nuclear Data Tables 9 (1971) 265

5) J. O. Newton, in Nuclear Spectroscopy and Reactions, Part C, Ch. VIIE, ed. by J. Cerny, Academic Press (1974)

6) P. K. Hopke, H. Hubel, R. A. Naumann, E. H. Spejewski and A. T. Strigachev, Nucl. Phys. A184 (1972) 497

7) G. Andersson, E. Arbman and B. Jung, Ark. Fys. 11 (1957) 297

8) K. Kumar and M. Baranger, Nucl. Phys. A110 (1968) 529

9) J. E. Blomqvist, Nuclear Theory Group Progress Report, State University of New York at Stony Brook, p. 29 April (1969), and private communication, June, 1969

10) K. Nakai, Phys. Letters 34B (1971) 269

11) F. S. Stephens, R. M. Diamond, D. Benson, Jr., and M. R. Maier, Phys. Rev. C7 (1973) 2163

12) R. F. Petry, R. A. Naumann, and J. S. Evans, Phys. Rev. 174 (1968) 1441

13) T. Inamura, Y. Tendow, S. Nagamiya and A. Hashizume, J. Phys. Soc. Jap. 32 (1972) 1163

14) J. C. Cunnane, R. Hochel, S. W. Yates, and P. J. Daly, Nucl. Phys. A196 (1972) 593

15) M. Ishihara, Nucl. Phys. A179 (1972) 223

16) K. Krien, E. H. Spejewski, R. A. Naumann, and H. Hübel, Phys. Rev. C5 (1972) 1751

17) M. Pautrat, G. Albouy, J. C. David, J. M. Lagrange, N. Poffé, C. Roulet, H. Sergolle, J. Vanhorenbeek, and H. Abou-Leila, Nucl. Phys. A201 (1973) 449.

18) F. Djadali, K. Krien, R. A. Naumann and E. H. Spejewski, Phys. Rev. C8 (1973) 323

19) C. M. Lederer, J. M. Hollander, and I. Perlman, Table of Isotopes (1967), Wiley

20) S. G. Nilsson, Mat. Fys. Medd. Dan. Vid. Selsk. 29 (1955) No. 16

TABLE 1. Transitions in ^{193}Tl

E_γ(keV)	I_γ[a]	$\alpha_K(90°)$	K/L(90°)	A_2	A_4	Confidence
96.8	5±1.5					A
107.9	5±1					C
125.9	8±1.5					A
161.6	6±0.7					A
202.3±0.3	3±0.4					C
207.9	4±0.5					A
268.9	10±1			-0.49±0.15	-0.02±0.15	A
316.6	17±1.2	0.20 ±0.05		-0.60±0.04	-0.01±0.04	A
320.9±0.3	12±1.4			-0.55± .02	0.06±0.02	A
323.7	28±3.2	0.21 ±0.05				A
365.3	43[b]			0.07±0.03	-0.03±0.03	A
392.3	100	0.11 ±0.025	6.5±1.6[c]	-0.74±0.02	0.02±0.02	A
406.3	31±2	0.12 ±0.03	4.6±0.8	-0.68±0.03	0.02±0.03	A
431.0	15±1.2	0.12 ±0.03	4.3±0.8	-0.51±0.08	-0.16±0.08	B
464.0	8±1			-0.56±0.05	0.02±0.05	C
466.8	19±2.5	0.09 ±0.025				A
469.7	5±1					C
672.5	21±2			0.18±0.07	0.00±0.08	B
716.2	40±3	0.0075±0.002		0.32±0.05	-0.02±0.05	B
735.6	48±3	0.006 ±0.0015		-0.19±0.04	0.04±0.04	A
741.6	9±2	0.03 ±0.015		0.24±0.17	-0.05±0.17	C
751.7	31±4	0.013 ±0.004		0.35±0.06	-0.14±0.06	B
754.4	23±2.7	0.011 ±0.004				B
790.0	6±1.6					C

[a] Where A_2 and A_4 coefficients are quoted, the intensities are corrected for the angular distributions. (In the three cases where two close-lying transitions were not fully resolved in the angular distribution measurements, the pairs of transitions were taken to have the same distributions. The data suggest that this would not be seriously in error.) In the other cases the intensities correspond to $[I_\gamma(90°)/I_{392}(90°)] \times 100$.

[b] This intensity depends on the duty cycle.

[c] Deduced from K/M + N + ... (the L line was obscured) assuming M + N + ... /L=0.3.

Table 2. Coincidence relationships between the ^{193}Tl γ-rays. The symbol Y indicates that the observed intensity is greater than three standard deviations σ above zero, whilst PY indicates that it is greater than 1.5 σ above zero. Absence of a symbol does not necessarily mean that a γ-ray is not in coincidence, it may simply indicate inadequate statistical accuracy.

	97	108	126	162	208	269	317	321	324	392	407	431	467	716	736
97			PY							Y	PY				
108										PY	PY				
126	PY			Y			PY			Y	Y		Y		Y
162			Y				Y			Y	Y		Y		
208						Y			PY	PY					
269					Y			PY	PY	Y				PY	
317			PY	Y			Y			Y	PY		Y		
321						PY				Y		Y			
324					PY	PY				Y	PY				
392	PY	PY	Y	Y	PY	Y	Y	Y	Y		Y	PY	Y		Y
407	PY	PY	Y	Y			PY		PY	Y					Y
431								Y		PY					
467			Y	Y			Y			Y					
716						PY									
736			Y							Y	Y				

Table 3. Transitions in ^{195}Tl

E_γ(keV)	I_γ^a	A_2	A_4	Confidence
117.1	14±4			C
215.9	5±0.8			C
305.8	6±1.5			C
311.7±.25	17±5			C
313.2	35±5	-0.44±0.05	-0.05±0.05	A
316.6	14±2			B
383.7[b]	175±20	-0.04±0.10	0.02±0.11	A
394.2	100	-0.64±0.04	0.06±0.04	A
492.1	25±3	-0.30±0.12	0.27±0.14	B
458.9	23±3	-0.51±0.16	0.18±0.17	B
607.6	16±4	-0.10±0.16	-0.10±0.17	A
707.8	51±6	0.28±0.09	-0.19±0.09	A
742.5	10±3			C
821.9	8±3	0.3 ±0.5	0.2 ±0.5	C
848.1	29±5	0.01±0.16	0.25±0.17	B

[a] The intensities are evaluated as in Table 1.

[b] Includes between beam-intensity.

Table 4. Transitions in ^{195}Pb decay

E_γ(keV)	I_γ	α_K	Coinc.	Multipol.	Confidence
313.4	15.5±1.5	0.27	394	M1	A
383.7	243 ±4	0.069[a]		E2 + M1	A
394.2	100	0.14	313,607	M1	A
493.2±0.6	5 ±1			M1	C
534.1	5 ±1				C
581.6	8 ±1	0.022±.006		M1(+E2)	C
607.5	21 ±2	0.027	394	M1(+E2)	A
630.4	7 ±1				C
691.2	6 ±1				C
707.6	31 ±3	0.009		E2	A
741.9	7 ±2				C
848.2	8 ±1				C
878.2	55 ±5	0.008		E2	A

[a]By definition.

Table 5. Transitions in ^{197}Tl

E_γ (keV)	I_γ (90°)	Confidence
152.5	7 ±1.5	B
171.2	14 ±4	B
205.8	8 ±3.5	B
219.5	4.1±0.8	C
222.4	17 ±1.3[a]	A
263.3	18 ±2.4	C
298.6	3.5±1.3	C
307.7	16 ±1.6	A
385.7	43 ±4	A
387.7	100	A
407.7	8 ±1.2	C
416.4	15 ±1.5	B
561.2	40 ±5	A
695.6	17 ±2.7	B
707.1	10 ±2	C
715.8	7 ±2	C
724.2	13 ±2	C
740	4.4±1.6	C

[a] Depends on duty cycle.

Table 6. Transitions observed in ^{197}Pb decay

This work			Hopke et al.[6]	
E_γ(kev)	I_γ	Confidence	E_γ(keV)	I_γ
222.4	24	A	222.4±0.3	22
239.5	4.5	B		
252.9	17	B		
290.4	1	C	290.4±0.4	0.8
307.7	5	B	308.0±0.4	
322.6	1	C	322.6±0.8	0.35
366.0	6	B		
375.3	3	C	375.3±0.4	12
385.7	100	A	385.6±0.4	129
387.7	29	A		
416.0	2	C	415.5±0.6	1.4
			558.0±0.9	4
			608.5±0.9	4
			695.0±1.0	13
			722.0±1.0	3
			761.0±1.1	7
			773.0±1.1	18

Table 7. Transitions in ^{191}Tl.

E_γ (keV)	I_γ (90°)	$I_\gamma(0°)/I_\gamma(90°)$	Confidence
306.4	24±3	$0.26^{+0.4}_{-0.2}$	B
313.0	13±2		C
325.6	32±3	0.24±0.1	B
387.6	100	0.25±0.08	A
405.0	36±3	$0.08^{+0.3}_{-0.08}$	B
427.8	16±3.5		C
434.5	20±4	$0.06^{+.3}_{-.06}$	C
614.2	40±5	$0.30^{+0.5}_{-0.2}$	B
713.2±0.6	24±6	$1.20^{+0.9}_{-0.4}$	C
730.0±0.7	15±5		C
749.6±0.7	19±4	$1.35^{+0.8}_{-0.4}$	C

Table 8. Ratios of energies of transitions in the proposed K = $9/2^-$ and $13/2^+$ rotational bands to those of the 2 → 0 and 4 → 2 transitions in the appropriate Hg core nuclei

K	$9/2^-$	$9/2^-$	$9/2^-$	$9/2^-$	$9/2^-$	$13/2^+$	$13/2^+$	$13/2^+$
E[K+1 → K] keV	369.3	387.7	394.2	392.3	387.6	(405.0)	406.3	(458.9)
E(0 → 2) keV	411.7	426.1	428.4	423.0	416.3	416.3	423.0	428.4
E(K+1→K)/E(0→2)	0.897	0.910	0.920	0.927	0.931	(0.973)	0.960	(1.071)
E(K+3→K+1) keV	748.5	724.2	742.1	754.5	(760.1)		592.7	
E(4→2) keV	636.8	635.3	636.8	634.7	625.1		634.7	
E(K+3→K+1)/E(4→2)	1.175	1.140	1.165	1.188	(1.216)		0.934	
A	199	197	195	193	191	191	193	195

Figure Captions

Fig. 1. Spectrum of in-beam γ-rays from the $^{181}Ta(^{16}O,4n\gamma)^{193}Tl$ reaction at 82 MeV bombarding energy.

Fig. 2. Spectrum of γ-rays in coincidence with the 392 keV γ-line from the $^{181}Ta(^{16}O,4n\gamma)^{193}Tl$ reaction.

Fig. 3. Spectrum of in-beam internal conversion electrons from the $^{181}Ta(^{16}O,4n\gamma)^{193}Tl$ reaction taken with the wedge-gap spectrometer. The positions of the K-, L- and M-lines of a few transitions are indicated.

Fig. 4. Level Scheme of ^{193}Tl. Transition intensities and most-probable assignments are shown. The levels of the suggested $13/2^+[606]$ band, shown by broken lines, were assigned partly from theoretical arguments (see section 4).

Fig. 5. Spectrum of in-beam γ-rays from the $^{188}Os(^{11}B,4n\gamma)^{195}Tl$ reaction at 57 MeV bombarding energy.

Fig. 6. Spectrum of γ-rays from ^{195}Pb decay taken for the first twelve minutes after bombardment.

Fig. 7. Spectrum of conversion electrons from ^{195}Pb decay taken between the beam pulses with a solenoidal electron spectrometer. The positions of the K-, L- and M-lines of a few transitions are indicated.

Fig. 8. Level Scheme of ^{195}Tl deduced from in-beam γ-ray measurements and from the decay of ^{195}Pb. Transition intensities and most probable assignments are shown.

Fig. 9. Spectrum of in-beam γ-rays from the $^{190}Os(^{11}B,4n\gamma)^{197}Tl$ at 57 MeV bombarding energy.

Fig. 10. Level scheme of ^{197}Tl deduced from in-beam γ-ray measurements and from the decay of ^{197}Pb. Gamma-ray intensities (90°) and most probable assignments are shown. Uncertain levels are indicated by broken lines.

Fig. 11. Spectrum showing the 386 and 388 keV γ-rays from ^{197}Pb decay.

Fig. 12. Spectrum of in-beam γ-rays from the ^{182}W(^{14}N,5nγ)^{191}Tl reaction at 93 MeV bombarding energy.

Fig. 13. Level scheme of ^{191}Tl. Gamma-ray intensities (90°) and most probable assignments are shown. The levels indicated by broken lines were assigned only on the basis of intensities, systematics and theoretical considerations (see Section 4).

Fig. 14. Energy systematics of levels in Hg and Tl nuclei. Level positions for Hg nuclei are connected by thick lines and for Tl nuclei by thin lines. Some levels, identified in the present work and in ref. 2, are shown by open circles and their proposed spins indicated.

Fig. 15. Estimated energies of high-spin levels in spherical odd-mass Tl nuclei (see text) are shown in the right and left sections, and partial level schemes for the nuclei ^{193}Tl and ^{199}Tl in the center. The estimated energies are shown by thick vertical lines with a spread of ±100 keV. The energies of the two-quasi-particle or collective states, in the doubly-even nuclei, are shown by thick horizontal lines with their assignments in round brackets. The assignments of the one-quasi-particle states with which they are combined are indicated by square brackets.

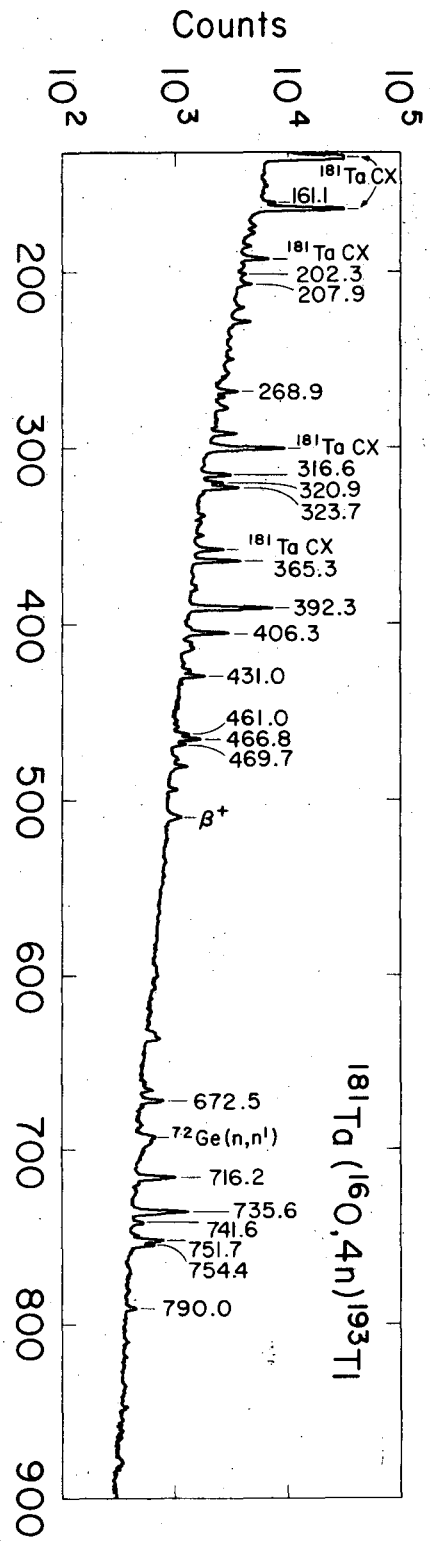
Counts
10^2
10^3
10^4
10^5
200
300
400
500
600
700
800
900
Energy (keV)
^{181}Ta CX
161.1
^{181}Ta CX
202.3
207.9
268.9
^{181}Ta CX
316.6
320.9
323.7
^{181}Ta CX
365.3
392.3
406.3
431.0
461.0
466.8
469.7
β^+
672.5
^{72}Ge(n,n')
716.2
735.6
741.6
751.7
754.4
790.0
^{181}Ta (^{16}O,4n)^{193}Tl
XBL 744-2798

Fig. 1

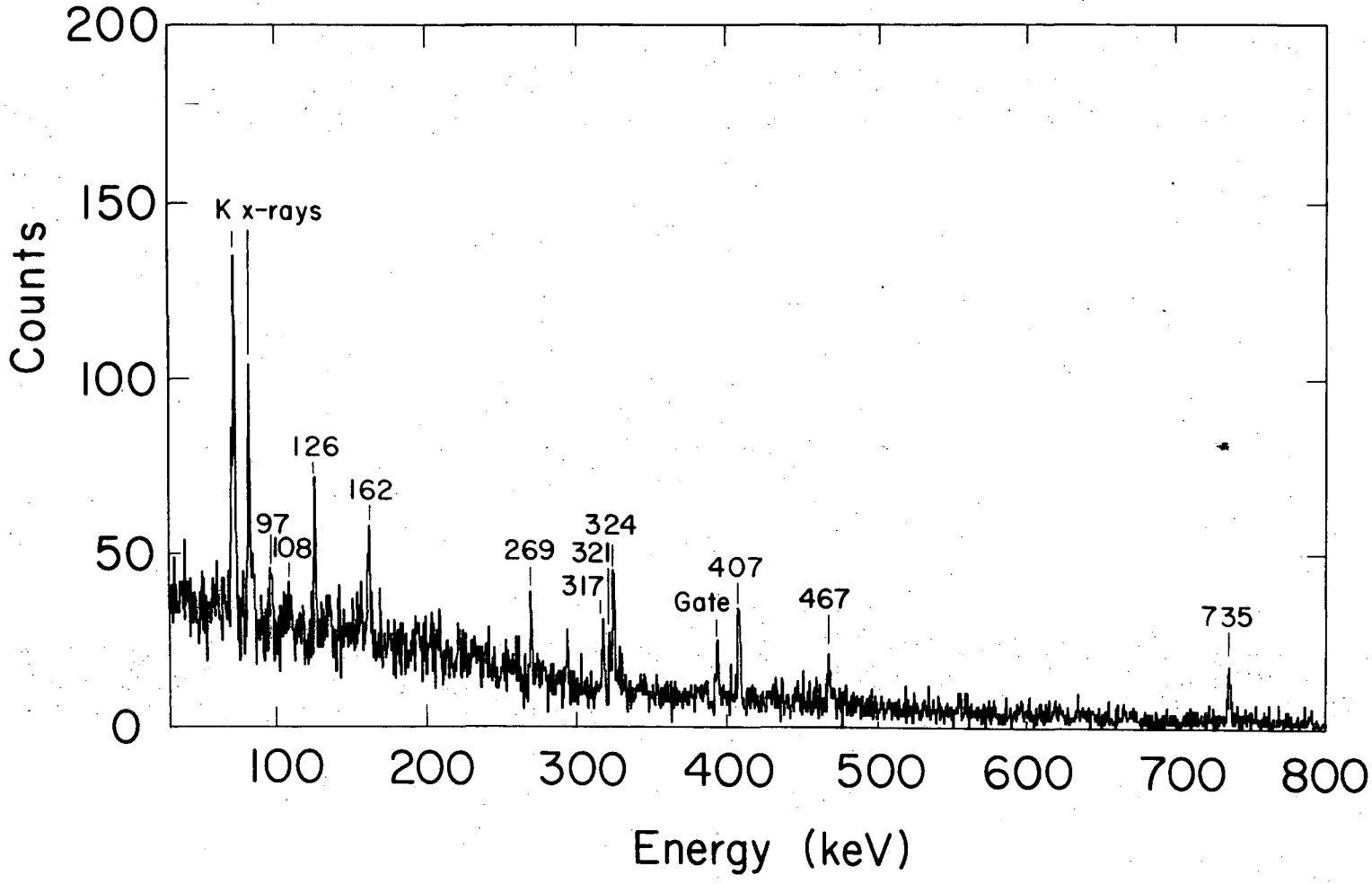
200
150
100
50
0
Counts
K x-rays
126
162
97
108
269
324
321
317
407
Gate
467
735
100
200
300
400
500
600
700
800
Energy (keV)
XBL 744-2797

Fig. 2

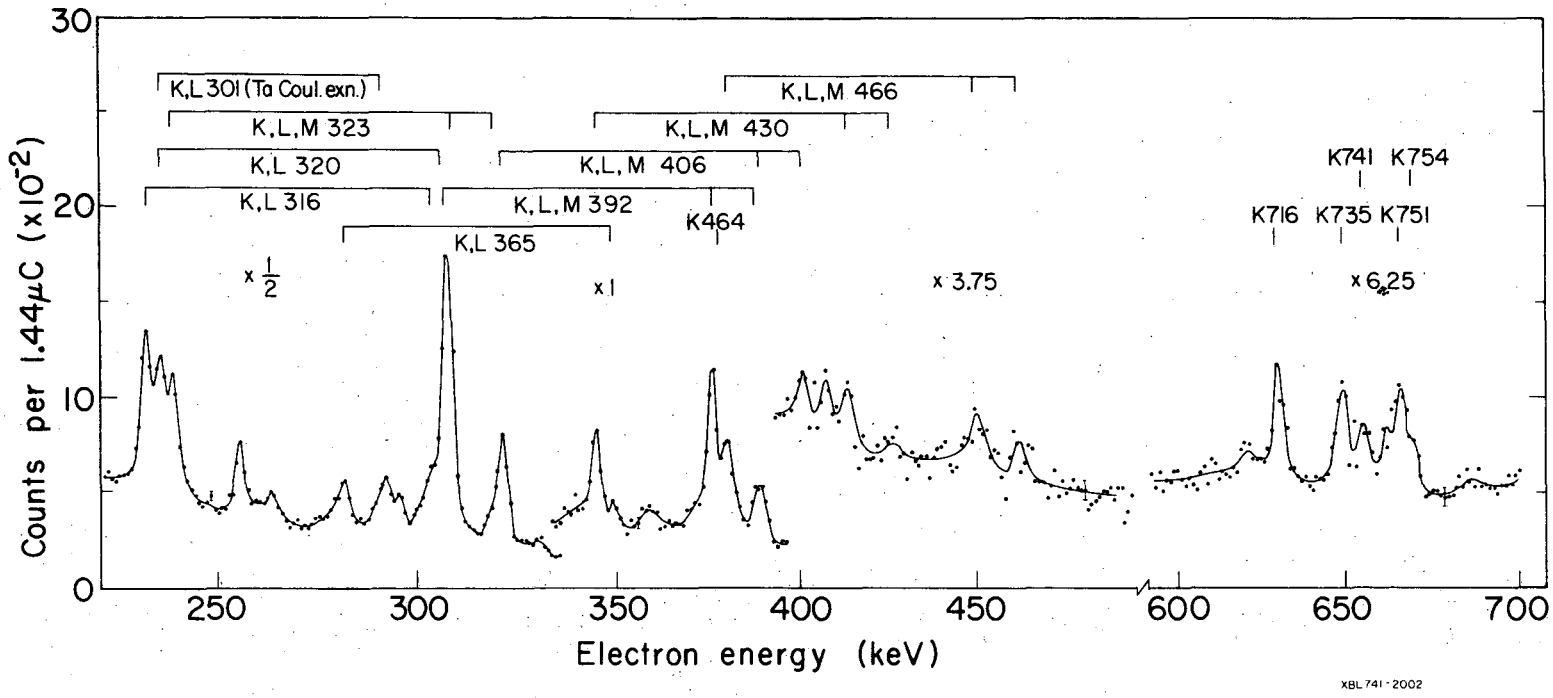
K,L 301 (Ta Coul. exn.)
K,L,M 323
K,L 320
K,L 316
K,L 365
K,L,M 392
K464
K,L,M 406
K,L,M 430
K,L,M 466
K741 K754
K716 K735 K751
x 1/2
x 1
x 3.75
x 6.25
Counts per 1.44μC (x10^-2)
Electron energy (keV)
XBL 741-2002

Fig. 3

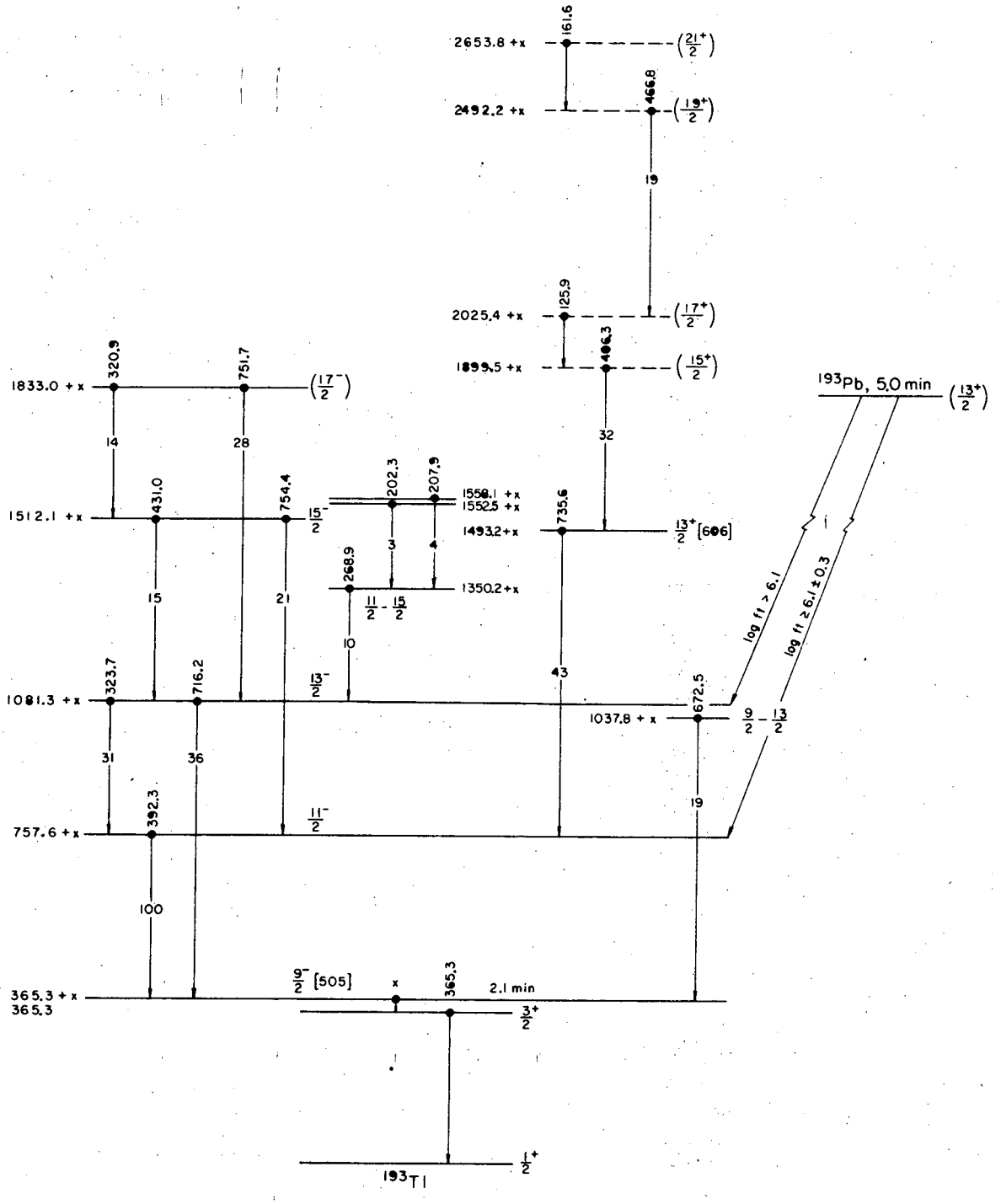

XBL741-2000

Fig. 4

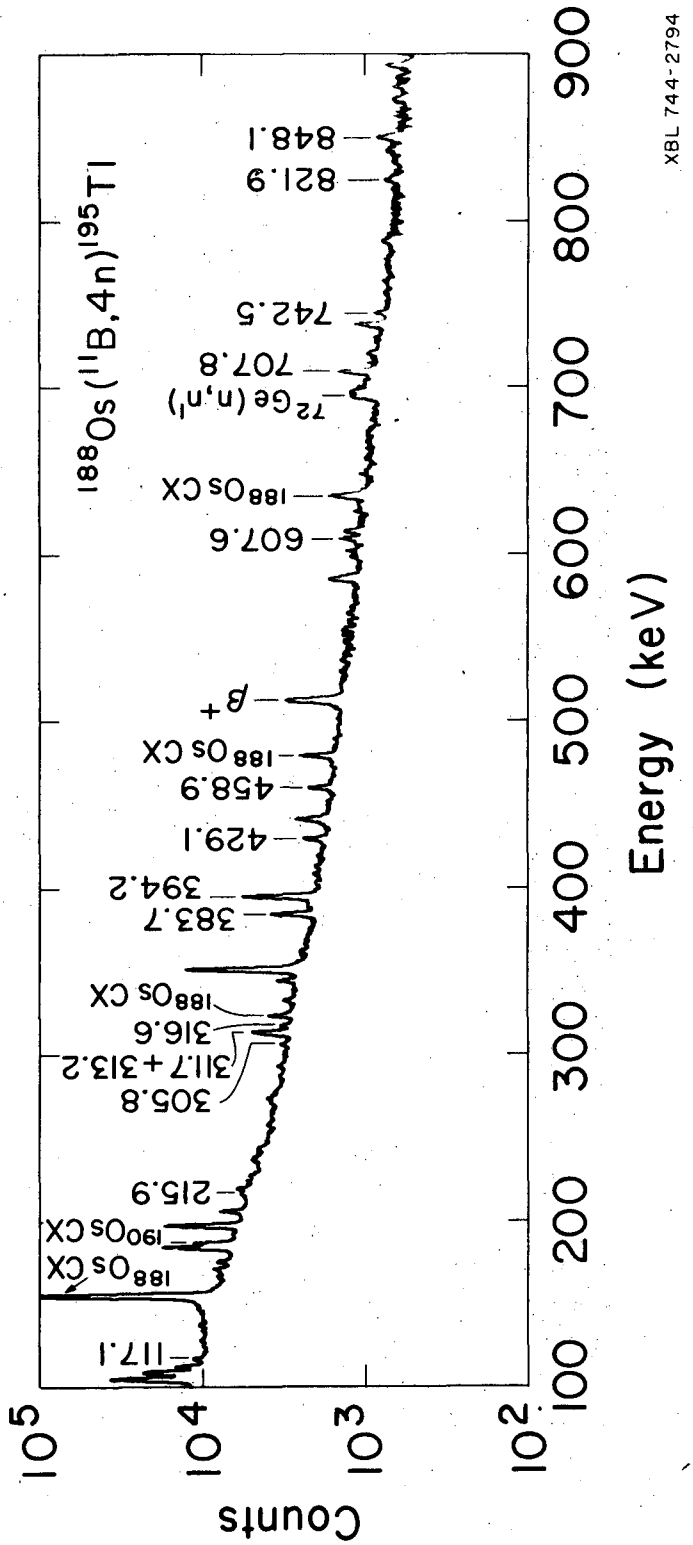
$^{188}Os(^{11}B,4n)^{195}Tl$
117.1
188Os CX
190Os CX
215.9
305.8
311.7 + 313.2
316.6
188Os CX
383.7
394.2
429.1
458.9
188Os CX
β+
607.6
188Os CX
72Ge (n,n')
707.8
742.5
821.9
848.1
Counts
Energy (keV)
XBL 744-2794

Fig. 5

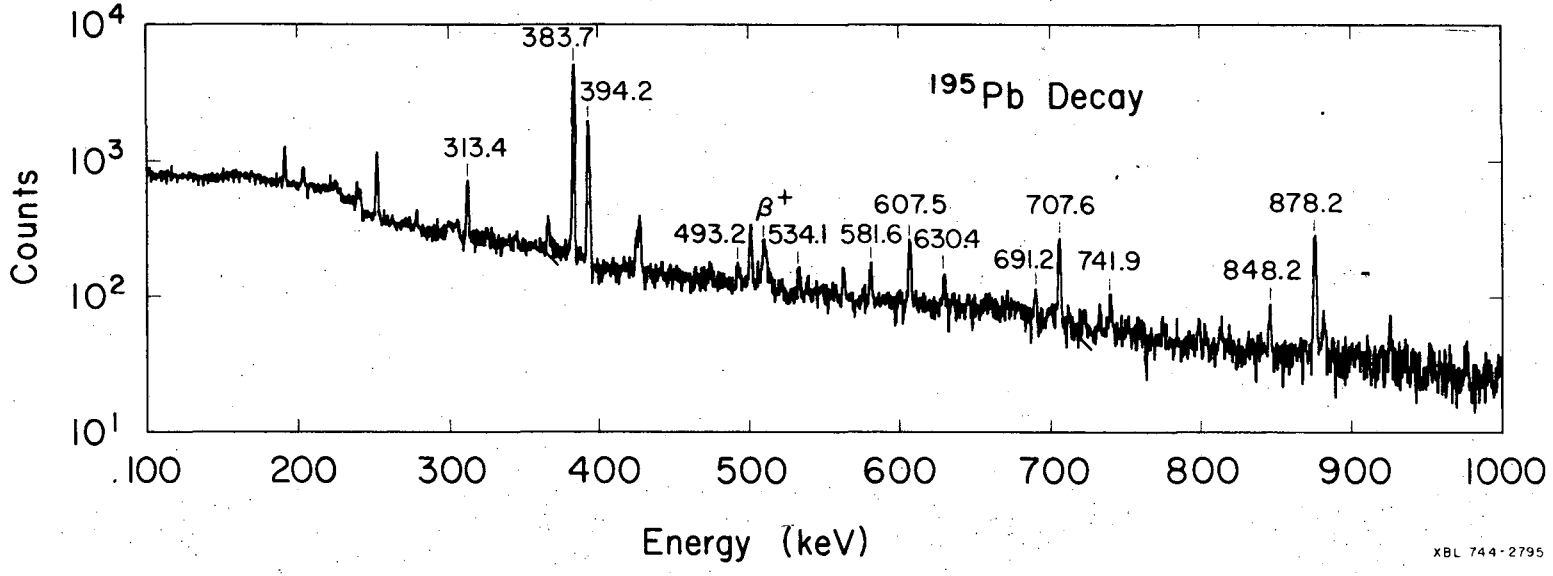
10^4
10^3
10^2
10^1
Counts
383.7
394.2
313.4
^{195}Pb Decay
β^+
493.2
534.1
581.6
607.5
630.4
691.2
707.6
741.9
848.2
878.2
100
200
300
400
500
600
700
800
900
1000
Energy (keV)
XBL 744-2795

Fig. 6

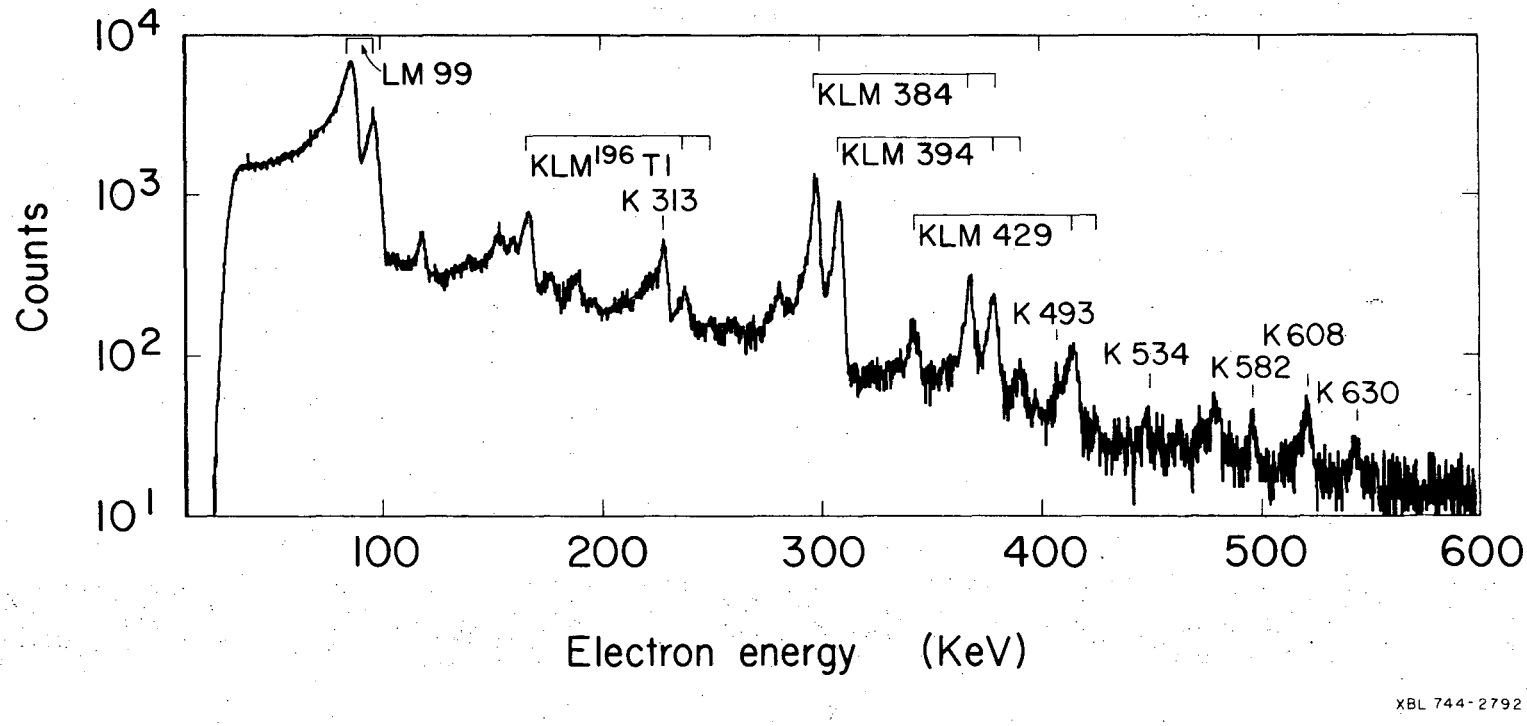
Counts
10^4
10^3
10^2
10^1
LM 99
KLM ^{196}Tl
K 313
KLM 384
KLM 394
KLM 429
K 493
K 534
K 582
K 608
K 630
100
200
300
400
500
600
Electron energy (KeV)
XBL 744-2792

Fig. 7

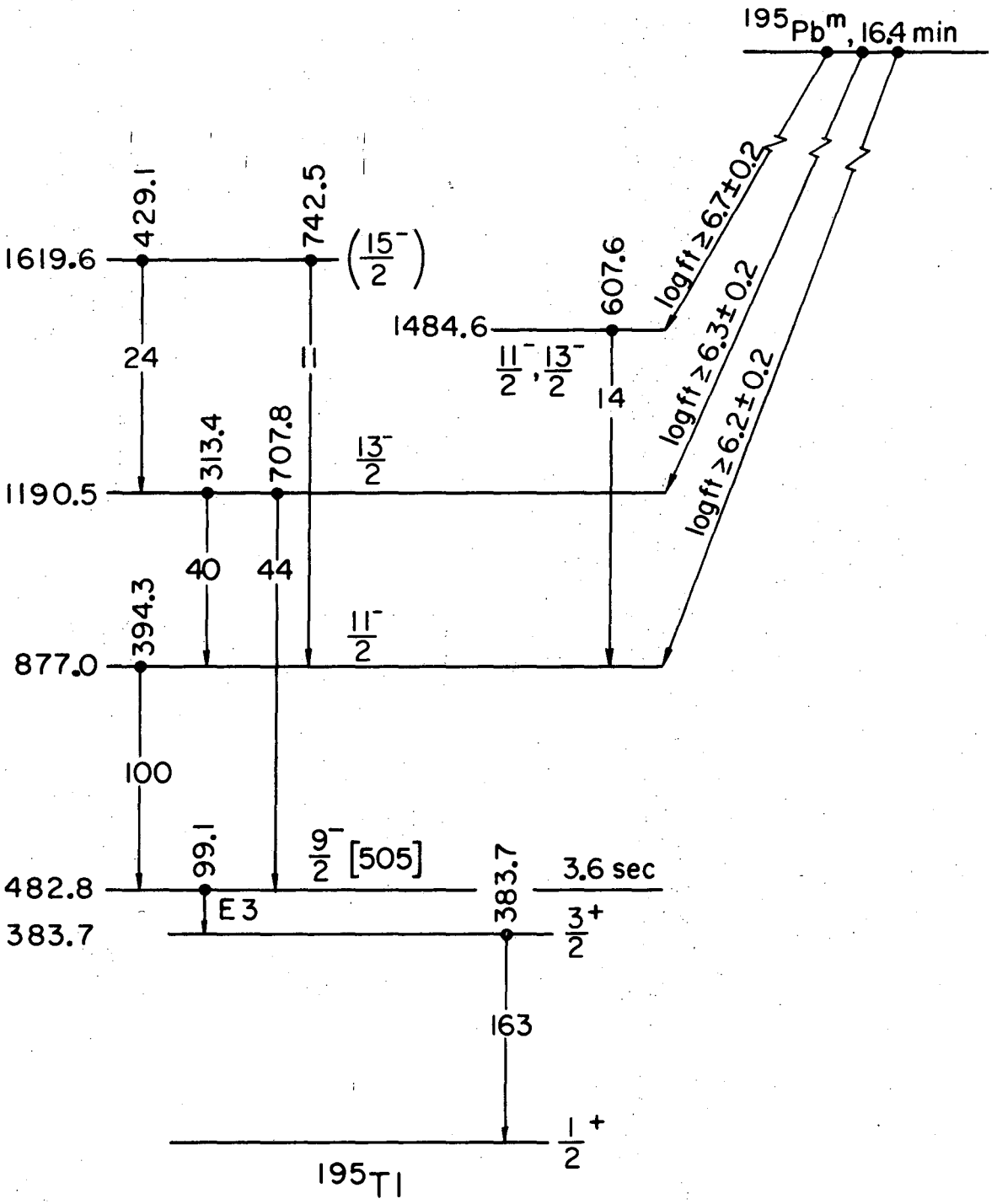

XBL 741-2006

Fig. 8

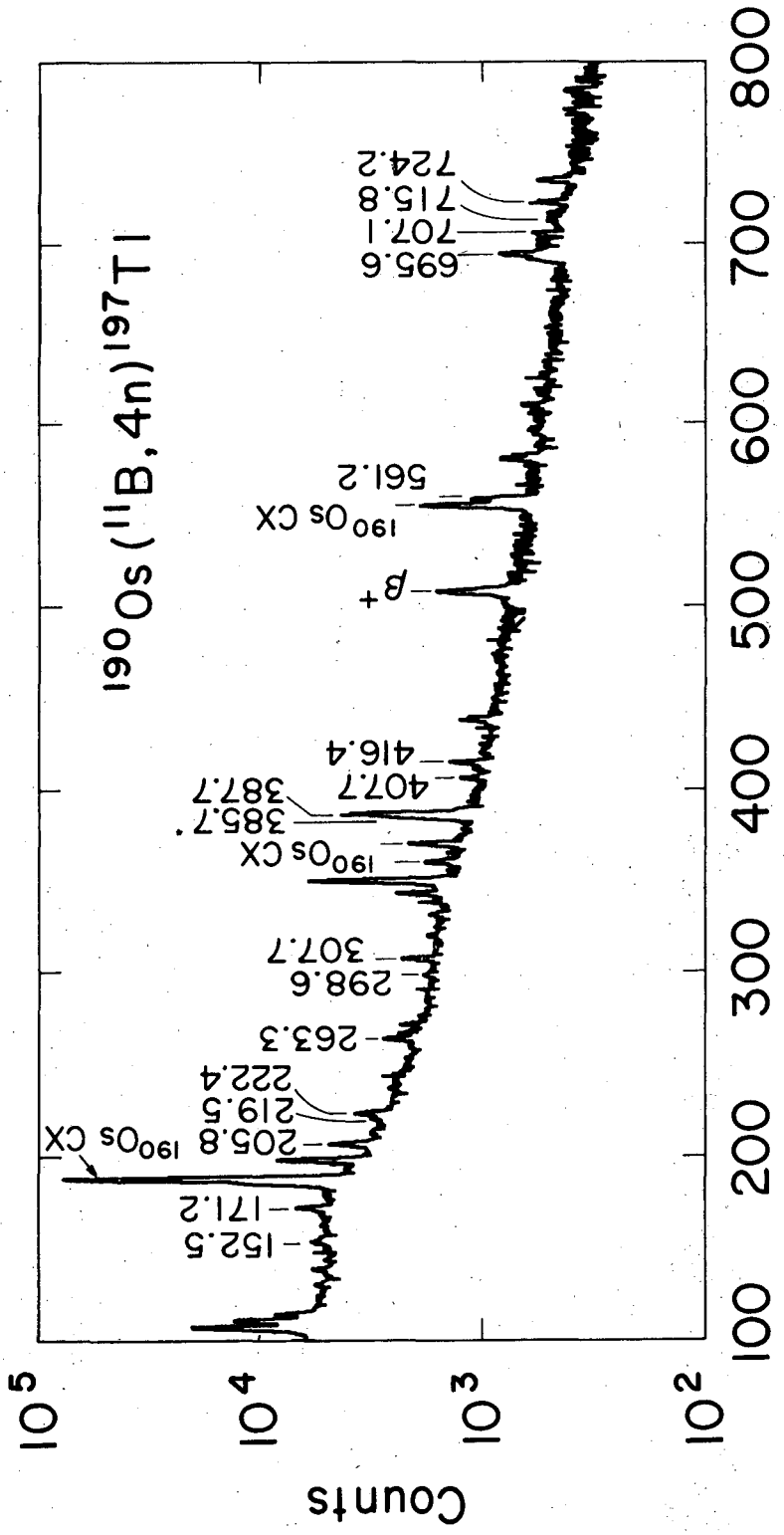

XBL 744-2793

Fig. 9

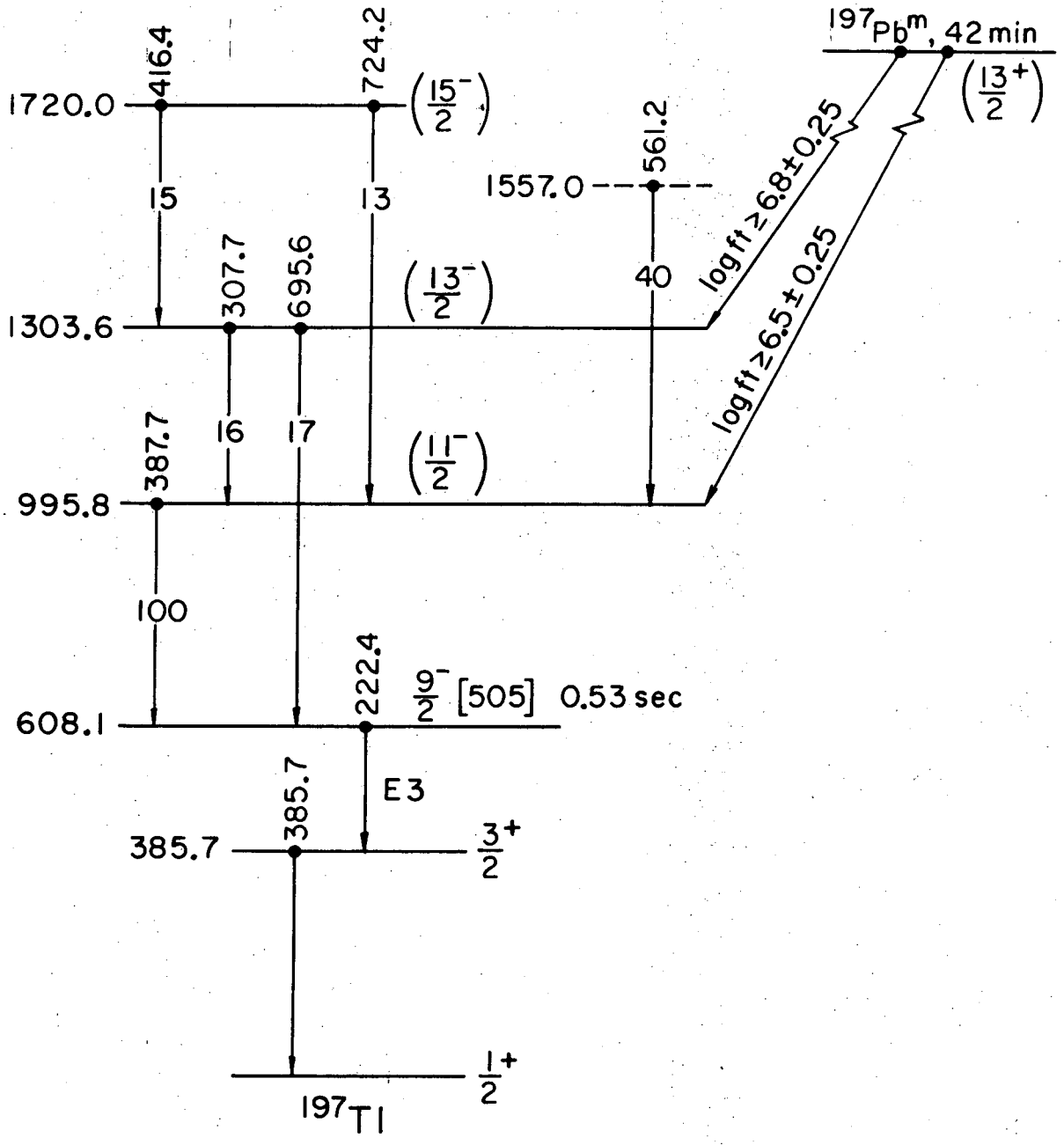

XBL741-2005

Fig. 10

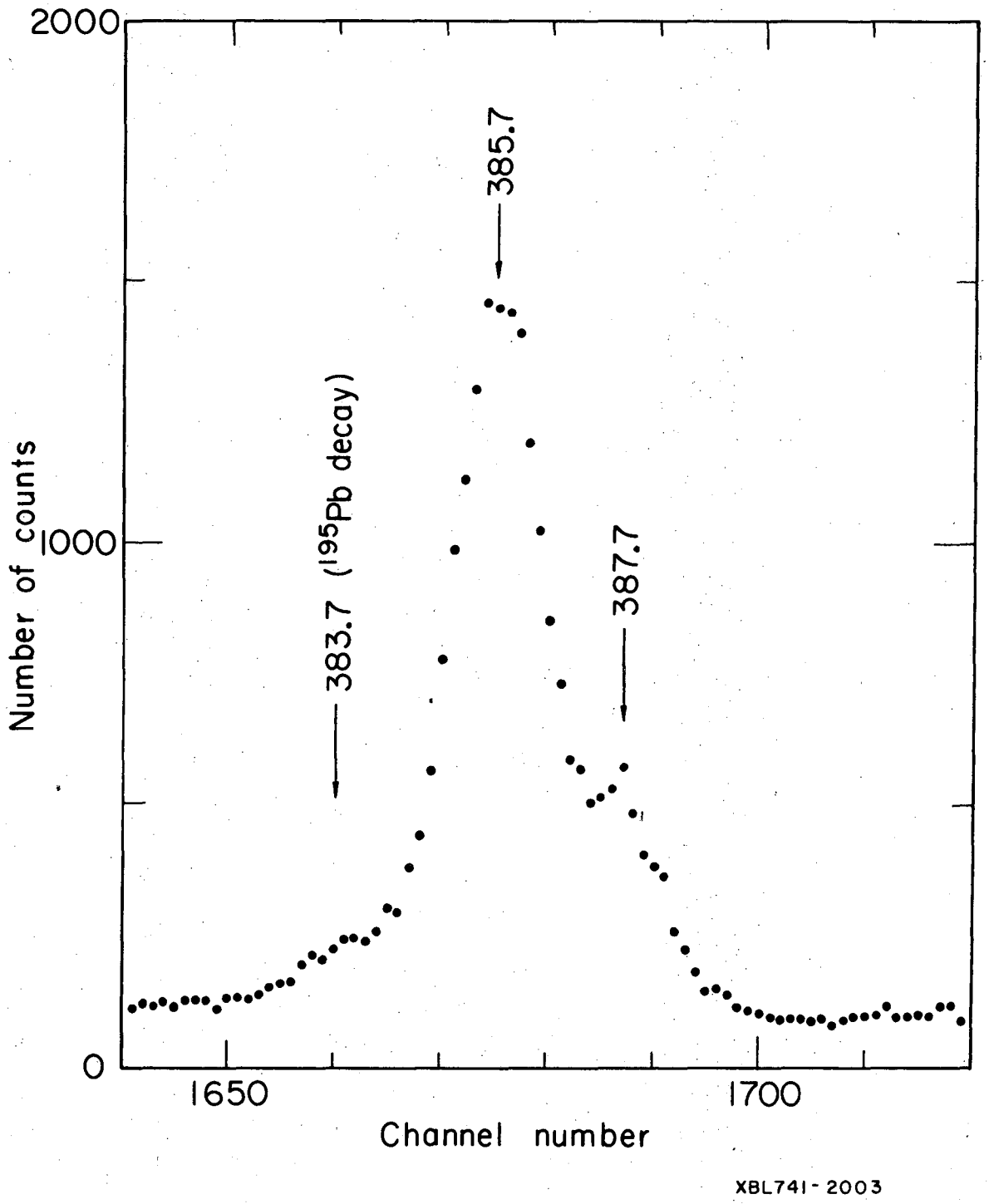
2000
1000
0
Number of counts
385.7
383.7 (^{195}Pb decay)
387.7
1650
1700
Channel number
XBL741-2003

Fig. 11

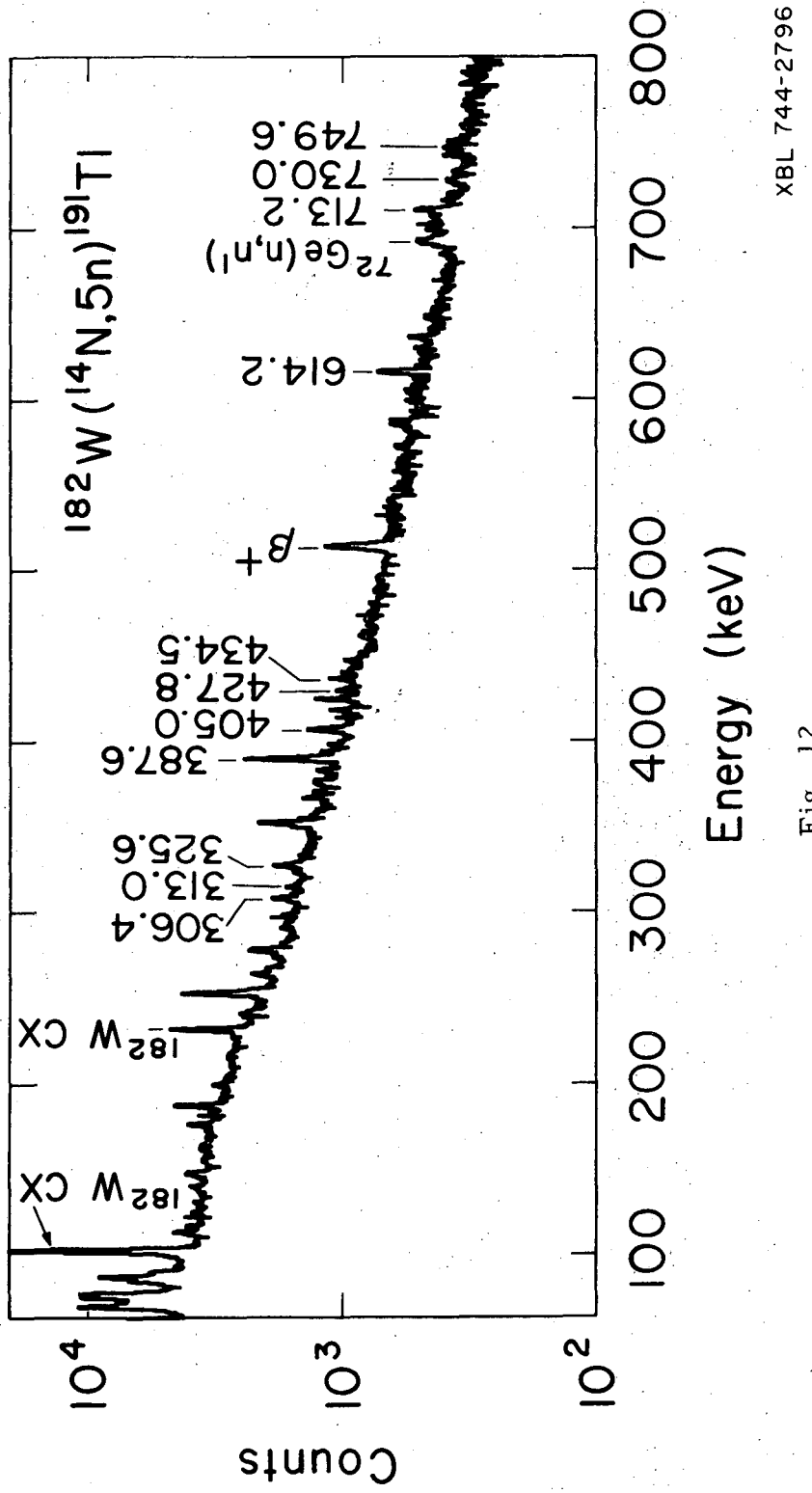

XBL 744-2796

Fig. 12

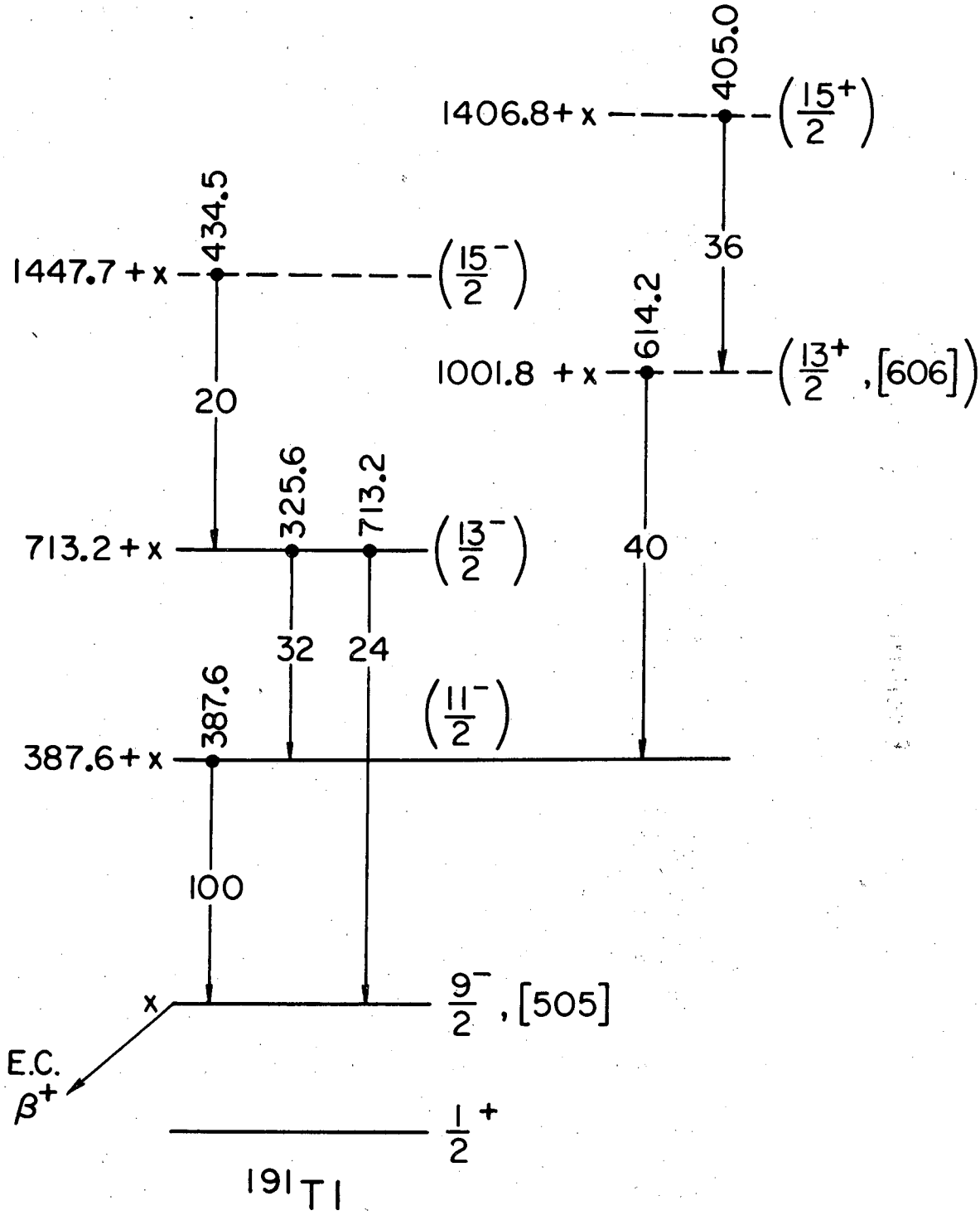

XBL 741-2007

Fig. 13

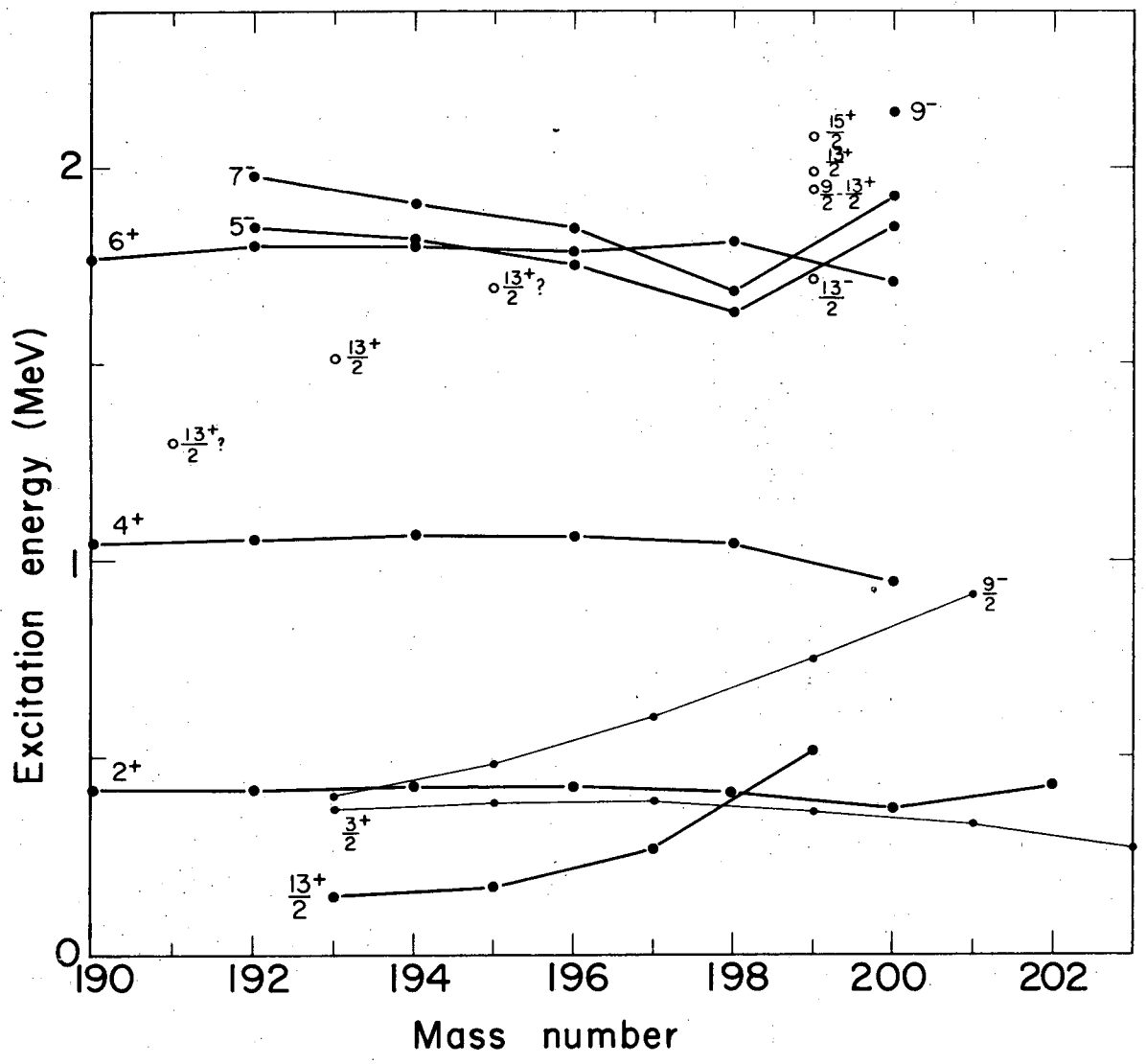
Excitation energy (MeV)
Mass number
0
1
2
190
192
194
196
198
200
202
6+
7−
5−
4+
2+
9−
15+/2
13+/2
9/2 - 13+/2
13−/2
13+/2 ?
13+/2
13+/2 ?
9−/2
3+/2
13+/2
XBL 741 - 2001

Fig. 14

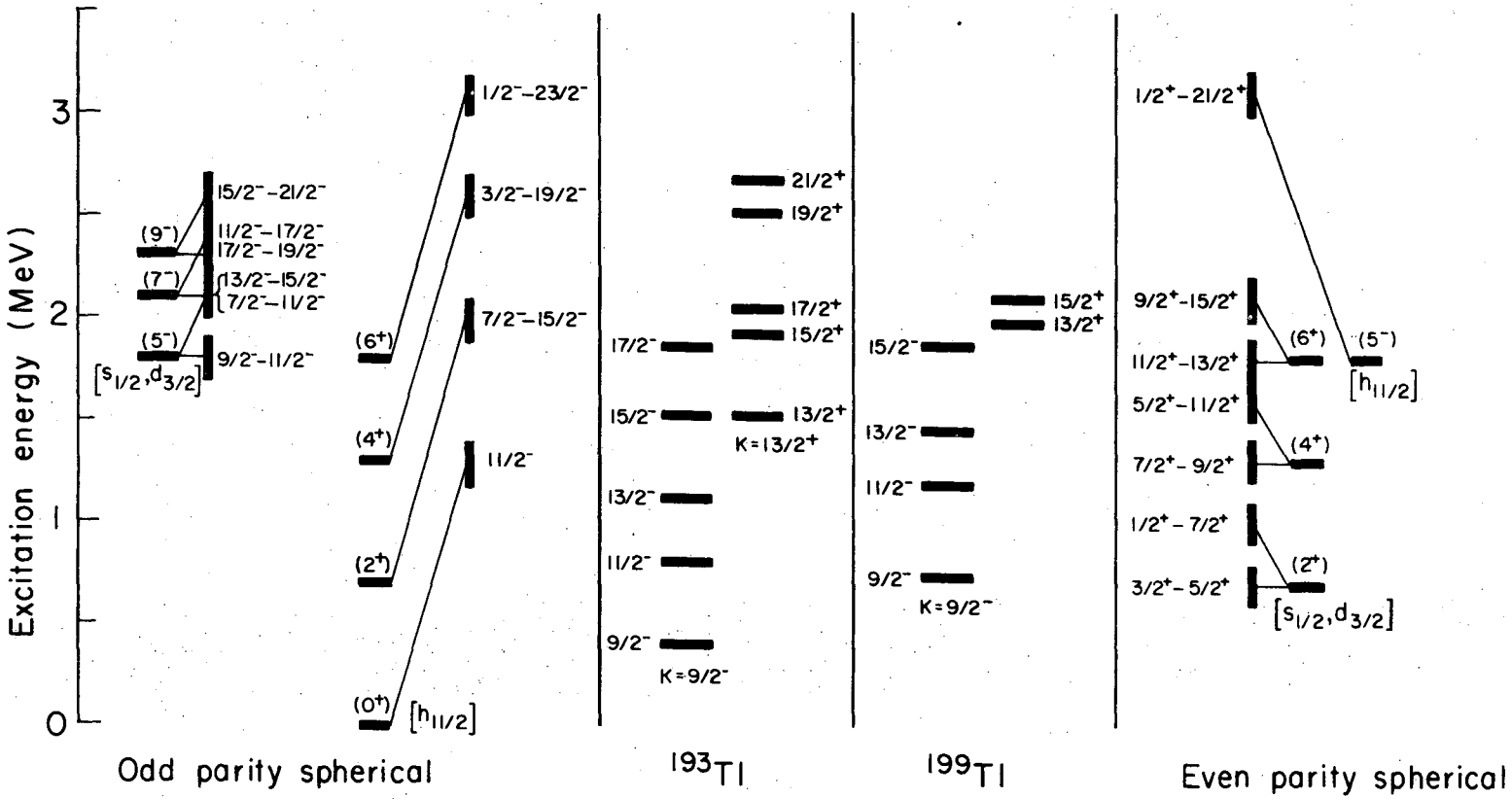

XBL741-2004

Fig. 15

LEGAL NOTICE

This report was prepared as an account of work sponsored by the United States Government. Neither the United States nor the United States Atomic Energy Commission, nor any of their employees, nor any of their contractors, subcontractors, or their employees, makes any warranty, express or implied, or assumes any legal liability or responsibility for the accuracy, completeness or usefulness of any information, apparatus, product or process disclosed, or represents that its use would not infringe privately owned rights.

TECHNICAL INFORMATION DIVISION
LAWRENCE BERKELEY LABORATORY
UNIVERSITY OF CALIFORNIA
BERKELEY, CALIFORNIA 94720